REPORT No. 915

EXTENSION OF USEFUL OPERATING RANGE OF AXIAL-FLOW COMPRESSORS BY USE OF ADJUSTABLE STATOR BLADES

By JOHN T. SINNETTE, JR., and WILLIAM J. VOSS

SUMMARY

A theory has been developed for resetting the blade angles of an axial-flow compressor in order to improve the performance at speeds and flows other than the design and thus extend the useful operating range of the compressor. The theory is readily applicable to the resetting of both rotor and stator blades or to the resetting of only the stator blades and is based on adjustment of the blade angles to obtain lift coefficients at which the blades will operate efficiently.

Calculations were made for resetting the stator blades of the NACA eight-stage axial-flow compressor for 75 percent of design speed and a series of load coefficients ranging from 0.28 to 0.70 with rotor blades left at the design setting. The NACA compressor was investigated with three different blade settings: (1) the design blade setting, (2) the stator blades reset for 75 percent of design speed and a load coefficient of 0.48, and (3) the stator blades reset for 75 percent of design speed and a load coefficient of 0.65. Most of the tests were conducted at an inlet-air pressure of 10.16 inches of mercury absolute and an inlet-air temperature of 0° F and extend over a range of compressor Mach numbers from 0.2 to 0.8 for the three blade settings. In order to investigate the effect of inlet-air conditions at low speeds, tests at a compressor Mach number of 0.2 were repeated for the first blade resetting with standard sea-level inlet-air conditions.

The experimental results show that a substantial increase in the useful operating range of axial-flow compressors can be obtained by adjustment of only the stator-blade angles. Considerable improvement in efficiency at compressor Mach numbers appreciably below the design value was obtained for both stator-blade resettings. A difference of 20 to 30 percent in the peak-efficiency flows for the two stator-blade resettings also was obtained, which at high compressor speeds was about seven times the maximum flow range for a particular blade setting. Peak pressure ratios were increased with the stator blades reset for a load coefficient of 0.65 and were substantially the same as for the design blade settings with the stator blades reset for a load coefficient of 0.48. Inlet-air conditions were found to have a very large effect on the adiabatic temperature-rise efficiency at low compressor Mach numbers, which is believed to be caused by heat-transfer and Reynolds number effects. No definite surging of the compressor was observed at Mach numbers lower than 0.4; instead a sudden transition to a lower pressure ratio occurred when the flow was decreased appreciably below the peak-efficiency point.

INTRODUCTION

The axial-flow compressor, in spite of the high peak efficiencies obtainable in modern designs (references 1 to 3), has had somewhat limited application because of its inherently narrow operating range. The useful flow range of a compressor at a given speed may be limited because of one or more of the following characteristics: (1) a rapid change in pressure ratio with a small change in flow; (2) a marked drop in the efficiency with changes of flow; and (3) unstable operation, referred to as "surging," which occurs when the flow is decreased beyond a certain point. The useful speed range of a compressor may be limited by a marked drop in peak efficiency with change in speed or by large differences between the peak-efficiency flow and the required flow at speeds appreciably different from the design speed. The characteristics that limit the useful range of axial-flow compressors are explained by the fact that the angles of attack, and hence the lift coefficients, for some of the blade rows are greatly affected by changes in flow and speed; some of the blade rows are therefore operating far from their optimum lift coefficients for speeds and flows appreciably different from the design.

An obvious remedy for these limitations on the useful range is to change the blade-angle settings with changes in operating conditions to maintain optimum lift coefficients. This method has been very successfully employed in extending the high-efficiency range of propeller turbines (references 4 and 5). Tests on axial-flow fans show that a very pronounced extension of the flow range can be obtained by the same method (references 6, pp. 100–104, 7, and 8). For high-speed multistage compressors, however, the adjustment of the many rows of rotor and stator blades during operation would involve mechanical problems of considerable difficulty. The alternative method of adjusting only the stator blades, which is mechanically more feasible, has been given particular consideration in the present investigation.

A general method of calculating blade-angle settings for a wide range of operating conditions has been developed. The method is applicable to the resetting of both rotor and stator blades or to the resetting of the stator blades alone and is based on the adjustment of blade angles to obtain lift coefficients at which the blades operate efficiently with special attention to the avoidance of blade stalling. Because of the extreme complexity of exact flow calculations, several simplifying approximations are made in the theoretical

analysis, of which the principal approximation is the assumption that conditions calculated at the mean radius represent the average conditions at each axial position. The flow is calculated by means of one-dimensional compressible-flow equations using an estimated polytropic exponent, the cross-sectional areas at the stations between each row of blades, and the air turning angle at the mean radius for each row of blades obtained from an empirical relation based on cascade tests.

The calculation method was applied to the resetting of stator-blade angles of the NACA eight-stage axial-flow compressor for 75 percent of design speed and for a series of load coefficients from 0.28 to 0.70. The load coefficient for peak efficiency at the design speed and for design blade setting was 0.64. The results of tests on the NACA eight-stage axial-flow compressor with design blade setting and with stator blades reset for 75 percent of design speed for load coefficients of 0.48 and 0.65 are presented. Most of the tests were conducted at an inlet-air pressure of 10.16 inches of mercury absolute (corresponding to a pressure altitude of 27,000 ft) and an inlet-air temperature of 0° F and extend over a range of compressor Mach numbers from 0.2 to 0.8. In order to determine the effect of inlet-air conditions at low compressor Mach numbers, tests with the blades reset for a load coefficient of 0.48 were repeated at a compressor Mach number of 0.2 with standard sea-level inlet conditions.

This theory was developed and experimentally verified at the NACA Cleveland laboratory during the summer of 1944.

SYMBOLS

The symbols used in this report are defined here in alphabetical order. Quantities that are a function of the radius are assumed to refer to the arithmetic mean radius, unless otherwise stated. Where the subscripts are not associated with the main symbol in the definition, the significance of the subscripts is given in the list following the main symbols.

A cross-sectional area of passage, square feet
a local velocity of sound, feet per second
B number of blades in row
C constant in Bernoulli's equation
C_L lift coefficient based on mean relative velocity
c blade chord, feet
c_p specific heat at constant pressure, Btu per pound per °F
c_v specific heat at constant volume, Btu per pound per ° F
D/L profile drag-lift ratio
g standard acceleration of gravity, 32.174 feet per second per second
J mechanical equivalent of heat, 778 foot-pounds per Btu
K constant in empirical relation for turning angle
m polytropic exponent for compression
m' polytropic exponent for expansion
n rotor speed, rps
P absolute total pressure, pounds per square foot
p absolute static pressure, pounds per square foot
Q volume rate of flow, cubic feet per second
Q_1/n load coefficient, cubic feet per revolution
$Q_1/\sqrt{\theta}$ equivalent volume flow (volume flow corrected to NACA standard sea-level temperature of 518.6° R), cubic feet per second
R gas constant, foot-pounds per pound °R
R_c compressor Reynolds number, $\frac{\rho_1 U_t c}{\mu_1}$
r radius to blade element, feet
T total temperature, °R
t static temperature, °R
U velocity of rotor ($2\pi rn$) at radius r, feet per second
U_t/a_1 compressor Mach number
u ratio of rotor velocity to axial component of air velocity, U/v
V absolute air velocity, feet per second
v axial component of air velocity, feet per second
W air velocity relative to rotor, feet per second
W_a air weight flow, pounds per second
w_m ratio of whirl component of air velocity (based on mean of inlet and outlet velocities relative to row of blades) to axial component of air velocity
Δw ratio of increase in relative whirl component to axial component of air velocity (normally negative)
α angle of attack measured between blade chord and entering air velocity, degrees
α_0 angle of attack at zero lift for isolated airfoil, degrees
β angle between compressor axis and absolute air velocity (referred to hereinafter as "air angle"), degrees
γ adiabatic exponent, c_p/c_v
δ ratio of inlet-air total pressure P_1 to NACA standard sea-level pressure $p_{s_l}=2116.2$ pounds per square foot
ζ loss ratio, ratio of power loss to power input by rotor (for a stage)
η blade-profile efficiency for stage, $1-\zeta$
η_p polytropic efficiency for compression
η_p' polytropic efficiency for expansion
η_T adiabatic temperature-rise efficiency (for constant γ),

$$\eta_T=\frac{T_1\left[\left(\frac{P_{20}}{P_1}\right)^{\frac{\gamma-1}{\gamma}}-1\right]}{T_{20}-T_1}$$

or

$$\eta_T=\frac{T_1\left[\left(\frac{P_{19}}{P_1}\right)^{\frac{\gamma-1}{\gamma}}-1\right]}{T_{19}-T_1}$$

θ ratio of inlet-air total temperature T_1 to NACA standard sea-level temperature, $t_{s_l}=518.6°$ R
μ absolute viscosity, pound-second per square foot
ρ mass density of air, slugs per cubic foot
σ blade-element solidity, $cB/(2\pi r)$ at radius r
ϕ angle between compressor axis and air velocity relative to rotor (referred to hereinafter as "relative air angle"), degrees
ψ angle between blade chord and axis of compressor, degrees

Subscripts:

1	ahead of compressor where velocity is negligible (figs. 1 and 2)
2	directly ahead of entrance guide vanes (fig. 1)
3	directly ahead of first row of rotor blades (fig. 1)
4	behind first row of rotor blades (figs. 1 and 2)
19	behind last row of stator blades (figs. 1 and 2)
20	in outlet pipe from compressor (fig. 2)
f	flow average
i	inlet to stator row of blades for any stage (i=4, 6, 8, . . .) (fig. 1)
$i+1$	inlet to following rotor row (fig. 1)
$i+2$	inlet to next stator row (fig. 1)
k	integer
m	mean of inlet and exit values for row of blades
mr	at mean radius
R	rotor
S	stator
st	standard
t	at rotor-blade tip (casing surface)
w	whirl component

BLADE-RESETTING THEORY

The general principles that are involved in the theory of blade resetting are discussed in the following section and the details of the method are presented in the section entitled "Method of Calculation." The procedure is illustrated by its application to the NACA eight-stage axial-flow compressor.

ANALYSIS OF PROBLEM

Effect of operating conditions on compressor performance.—The losses in any stage of an axial-flow compressor may be divided into losses resulting from blade profile drag, blade-end effects, and passage-wall friction. The profile efficiency at any given radius depends on the profile drag-lift ratio and the ratio of the various velocity components, as given by the following equation:

$$\eta=1-\frac{\left(\frac{D}{L}\right)_R(1+w_{m,R}^2)}{u\left[1+\left(\frac{D}{L}\right)_R w_{m,R}\right]}-\frac{\left(\frac{D}{L}\right)_S(1+w_{m,S}^2)}{u\left[1+\left(\frac{D}{L}\right)_S w_{m,S}\right]}\frac{\Delta w_S}{\Delta w_R} \quad (1)$$

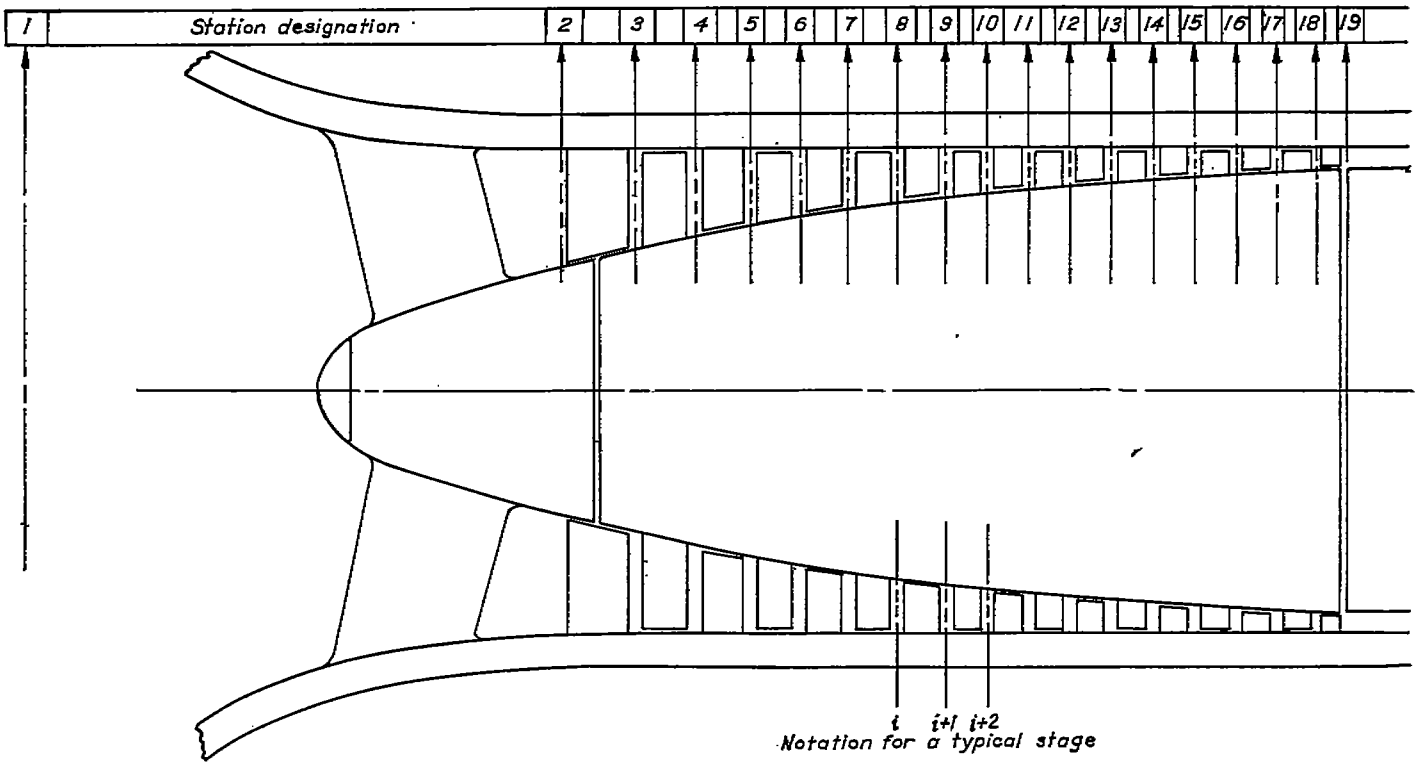

FIGURE 1.—Station designations used in calculations.

which is essentially the same as equation (11) of reference 1 but is generalized to allow for cases where Δw is different in the rotor and the stator, as may occur when the compressor is not operating at design conditions. It is obvious from equation (1) that, for high profile efficiency, $(D/L)_R$ and $(D/L)_S$ must be kept small.

The value of D/L depends, among other things, upon the lift coefficient at which the blades are operating and is generally a minimum at a lift coefficient somewhat below the stalling point of the blades. When the angle of attack is increased beyond the stalling point, the drag-lift ratio increases very rapidly with a corresponding decrease in profile efficiency. In order to obtain good efficiency, it is therefore important to avoid stalling the blades whenever possible. Because of blade-end effects and passage-wall friction, the over-all efficiency of a stage is less than the

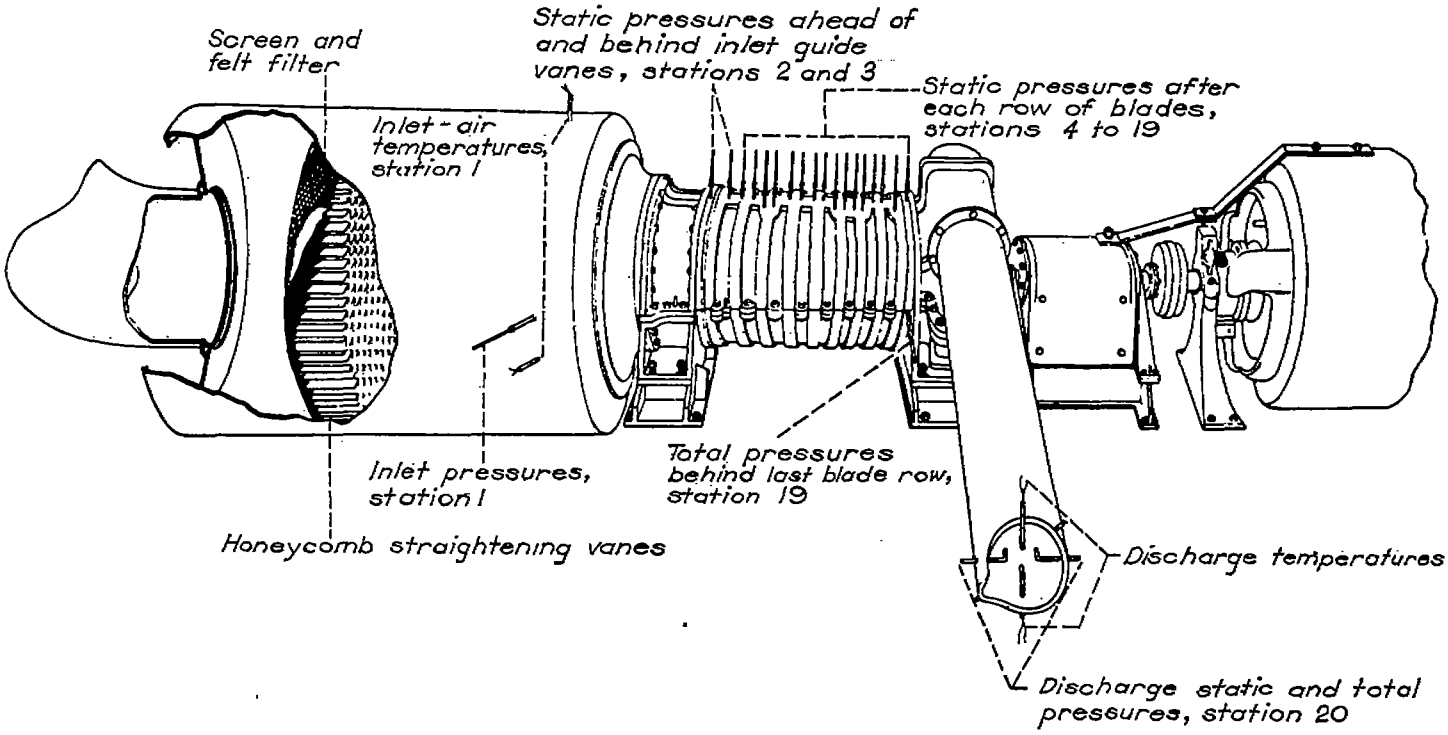

FIGURE 2.—Compressor setup showing location of pressure- and temperature-measuring stations. (Lagging removed.)

efficiency based on the profile drag of the blade elements. Inasmuch as tip-clearance losses are proportional to the square of the lift coefficient (reference 9), the lift coefficient that gives best over-all efficiency may be somewhat less than that indicated by profile efficiency; the difference depends upon blade aspect ratio and blade-tip clearances.

In a well-designed axial-flow compressor, all the blades will operate in the high-efficiency range of lift coefficients at the design operating condition; at speeds and flows differing appreciably from the design values, however, most of the blades will operate at unfavorable angles of attack, which will result in large losses. The effects of changes of flow on the angle of attack of a typical stage are shown in figure 3. In order to emphasize the main effects of changes of flow, the actual flow conditions have been somewhat simplified; the axial velocity and the radius to the element have been assumed constant throughout the stage. It is evident from figure 3 that a decrease in flow results in an increase in the angles of attack of both rotor and stator rows of blades, whereas an increase in flow produces the opposite effect. Either change, if excessive, results in a large increase in the drag-lift ratio and a corresponding decrease in efficiency. This effect of changes of flow on angle of attack is present in all stages of a multistage compressor but the additional effect of density changes throughout the compressor makes multistage compressors much more sensitive to changes of flow than single-stage units.

An increase in flow, for example, reduces the angle of attack and, in general, the density rise over a stage. As this decrease in density means that the axial velocity after the stage must increase more than ahead of the stage, the change in angle of attack and density rise in the second stage will be greater than in the first stage. This amplification process continues throughout the compressor with the result that small changes in flow at the inlet to a compressor may produce very large changes in axial velocity and angles of attack in the last stages.

The effect of compressor speed on performance is quite different in a multistage compressor than in a single-stage unit because the large density changes occurring have a marked effect on the axial-velocity distribution from stage to stage. The ratio of the mean axial velocities v_{i+k}/v_i between any two stations, represented by the subscripts i and $i+k$, is determined by the continuity equation

$$\frac{v_{i+k}}{v_i}=\left(\frac{\rho_i}{\rho_{i+k}}\right)\left(\frac{A_i}{A_{i+k}}\right) \qquad (2)$$

In the design of the compressor, the ratio of the cross-sectional areas at any two stations is chosen to give the desired velocity ratios at the design operating conditions. Inasmuch as the density ratio depends upon the speed at which the compressor is operating, the velocity ratios and the angles of attack will be correct only for design conditions. From the foregoing discussion, it is evident that two principal factors affecting the performance of a multistage compressor are air flow and compressor speed. Dimensional analysis shows that these factors are satisfactorily represented for a particular compressor by the load coefficient Q_1/n and the compressor Mach number U_1/a_1. (See reference 1.)

Control of lift coefficients by blade resetting.—For operation at conditions other than design, the blade angles can be reset to give arbitrary angles of attack for each row of blades at some point along the span of the blade, for example, at midspan; the angles of attack at other radii, however, cannot be arbitrarily chosen because the twist of the blades would have to be changed. The spanwise variation in lift coefficient will depend on the compressor design and on the extent of the deviations from the design blade settings. A general statement of the magnitude of the variations is therefore impossible but the following two factors should be considered in making an estimate: (1) At the compressor inlet where the hub-tip diameter ratio is usually small and the blades are considerably twisted, appreciable changes in the radial variation of the velocity may occur in reestablishing equilibrium when the blade setting is changed; and (2) at the compressor outlet, the development of a boundary layer along the hub and the casing has an important effect on radial distribution of lift coefficients with a tendency to load the blades more toward the ends than in the middle. If conservative lift coefficients are chosen at midspan, lift coefficients at other radii should not be excessive and satisfactory efficiencies should be obtainable for moderate deviations from the design operating conditions.

When only the stator blades are reset, it is no longer possible to choose arbitrarily the angle of attack at midspan on both the rotor and stator blades. The stator-blade angles must be set to keep the lift coefficients on both the rotor and stator blades within reasonable limits and, in particular, below the stalling points of the blades. The principle underlying the method of adjustment of stator blades alone is that an increase in the blade angle for a given row of stator blades not only reduces the angle of attack, and hence the lift coefficient, on that row of blades but also on the following row of rotor blades. (See fig. 4.) Consequently, stalling of

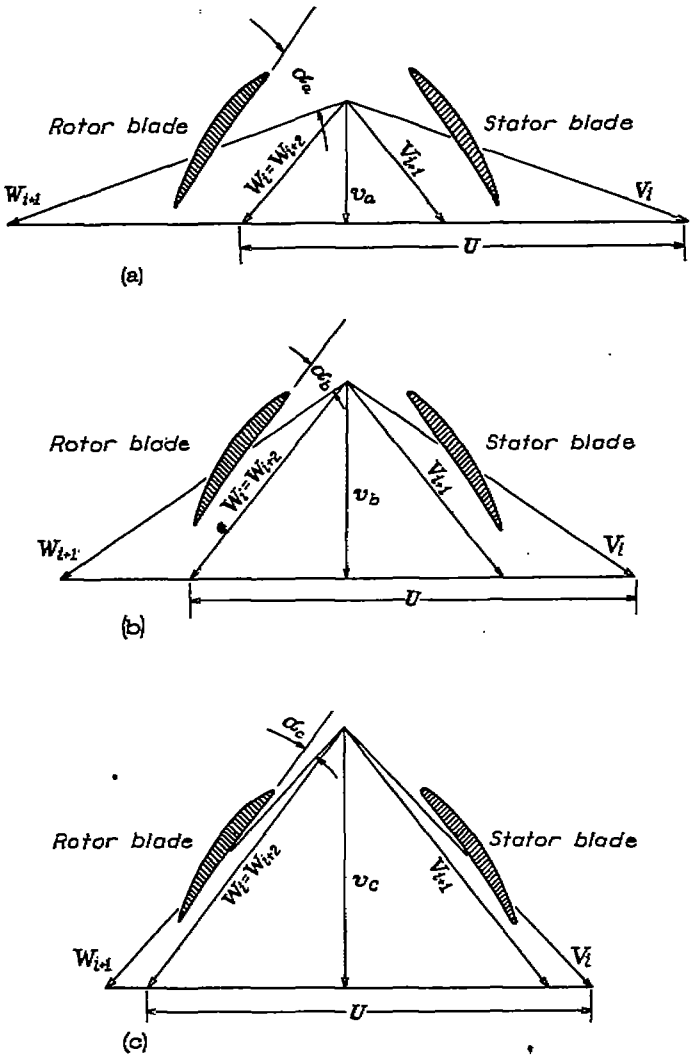

(a) Below normal flow: $v_a < v_b$; $\alpha_a > \alpha_b$.
(b) Normal flow.
(c) Above normal flow: $v_a > v_b$; $\alpha_c < \alpha_b$.

FIGURE 3.—Effect of flow on angle of attack for typical stage of axial-flow compressor.

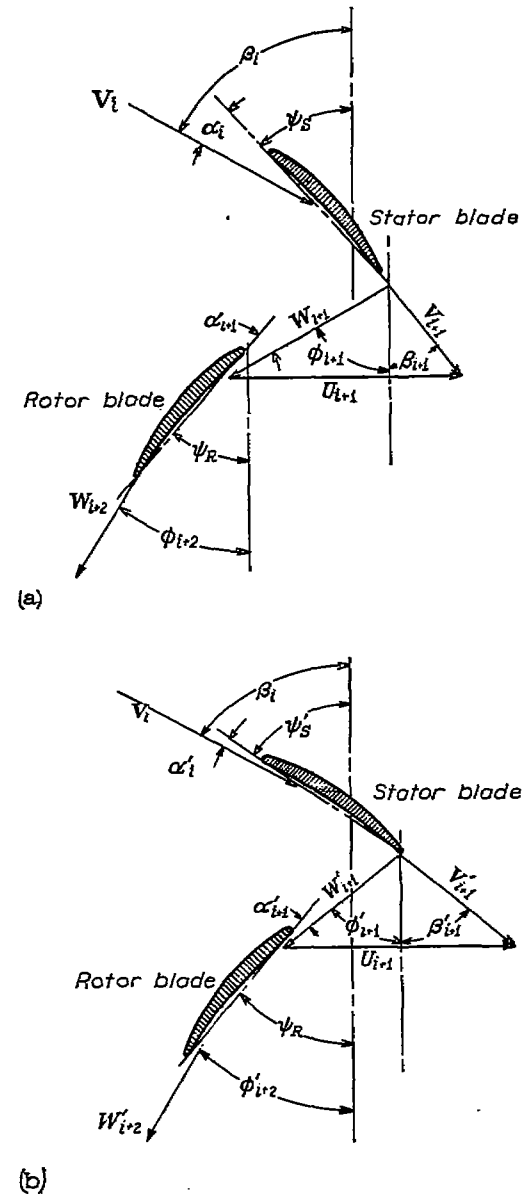

(a) Stator-blade angle, ψ_s.
(b) Stator-blade angle, $\psi_s' > \psi_s$.

FIGURE 4.—Effect of change in stator-blade angle on angles of attack for stator blades and following rotor blades.

either stator blades or rotor blades can be prevented by the adjustment of the proper row of stator blades: in the first case by the adjustment of the row of stator blades that are stalled; in the second case by the adjustment of the row of stator blades ahead of the row of stalled rotor blades.

Selection of lift coefficients.—The lift coefficient at which stalling occurs depends upon many factors, such as blade section, Reynolds number, solidity, blade-angle setting, and degree of turbulence. Experiments on airfoil cascades with retarded flow (reference 6, p. 75, and references 10 to 13) indicate that stalling occurs at appreciably lower lift coefficients than for isolated airfoils but there is some evidence (reference 14) that the lift coefficient at which stalling occurs on compressor blades is higher than for straight cascades. Because of the spanwise variation of lift coefficients and the lack of accurate information on the stalling of compressor blades, it would appear advisable to limit the maximum lift coefficient at midspan to about 0.8.

Special conditions at compressor inlet.—At the compressor inlet, the conditions are different because of the difference in function of the entrance guide vanes from that of the typical stator blades. The entrance guide vanes induce an initial whirl to the air in the direction of rotation of the rotor, whereas the typical stator row reduces the whirl component of the air velocity. When the compressor is operating at load coefficients appreciably below the design value, the angle of attack for the first rotor row becomes excessive. This condition can be somewhat alleviated by increasing the angle of the guide vanes with respect to the axis so as to increase the whirl component of the air entering the first rotor row. Only a limited improvement can be realized by this method for two reasons: (1) Stalling of the guide vanes may result if they are turned through a sufficient angle to prevent stalling of the rotor blades; and (2) turning of the guide vanes produces an appreciable shift in the radial distribution of axial velocity, which results in a very small change in angle of attack at the tip of the rotor blades for a large change in guide-vane angle. An example of the effect of guide-vane settings on the angles of attack and the lift coefficients at different radii on the first row of rotor blades is shown in table I, the values of which were calculated for the NACA eight-stage axial-flow compressor by the method given in appendix A.

Although little improvement in performance of the first row of rotor blades is obtainable by adjusting the guide-vane angles, acceptable over-all efficiencies may be obtainable in a multistage compressor when the first stage operates at low efficiency provided that the rest of the stages are operating at high efficiency.

Mach number limitations.—When the local relative Mach number at the entrance to a row of blades appreciably exceeds a certain value, referred to as the "critical Mach number," large compression-shock losses may result. For a given compressor Mach number U_t/a_1, any change in blade-angle settings will alter the velocity diagrams and, hence, the local Mach numbers through the compressor. When the compressor is operating near the design speed, the local Mach numbers on many of the blades will be near the critical values, and changes in blade-angle settings (especially changes that make the velocity diagrams asymmetrical) may cause the critical Mach numbers on some of the blades to be exceeded. At high compressor speeds, changes in blade angles required to produce large changes in the flow may therefore lead to appreciable compression-shock losses. On the other hand, the useful flow range for a single blade setting may be extremely narrow at these high compressor speeds. Consequently, the extension of useful flow range by using different blade settings may be large compared with the range for a single blade setting. At low compressor speeds, factors other than compression shock will usually determine how much extension of useful flow range is possible by blade adjustment.

METHOD OF CALCULATION

For the determination of blade resettings for particular operating conditions (given in the form of compressor Mach number and load coefficient), flow conditions and blade resettings are calculated progressively from the inlet to the outlet of the compressor. The stations at which flow conditions are calculated are taken midway between the various rows of blades as well as immediately ahead of the entrance guide vanes and after the last row of blades. The station designations used in the presentation are shown in figure 1. Unless otherwise stated, all flow conditions and blade angles refer to radii midway between the hub and the casing.

Because the entrance guide vanes have a function essentially different from that of the typical row of stator blades, the calculation procedure for the entrance guide vanes is treated separately from that of the typical stage. When the stator blades alone are reset, it is necessary to reset the entrance guide vanes only when the load coefficient for which the blades are reset is appreciably different from the design value. The most desirable guide-vane setting may be determined by calculating the lift coefficient on the first row of rotor blades for several guide-vane settings within the unstalled range of these vanes. (See appendix A.) For a typical stage (consisting of a row of stator blades followed by a row of rotor blades), the calculations are carried out for different stator-blade-angle settings until satisfactory lift coefficients are obtained on both the stator and rotor blades.

If both the stator and rotor blades are to be reset, adjustment of the entrance guide vanes is unnecessary unless it is desired to obtain a more favorable radial distribution of lift or a more symmetrical velocity diagram in the first stage. The calculations for the rest of the compressor are then carried out on a row of blades at a time using several blade-angle settings on each row until a satisfactory lift coefficient is obtained on the row.

Calculation procedure for entrance guide vanes.—For any given guide-vane setting, the flow conditions between the entrance guide vanes and the first row of rotor blades (station 3, fig. 1) are calculated by the following procedure: The

value of Q_1/a_1 is determined from the compressor Mach number U_t/a_1 and the load coefficient Q_1/n or from the flow corrected to standard sea-level temperature $Q_1/\sqrt{\theta}$ or $\frac{W_a\sqrt{\theta}}{\delta}$ by the relation

$$\frac{Q_1}{a_1}=\left(\frac{U_t}{a_1}\right)\left(\frac{Q_1}{n}\right)\frac{1}{2\pi r_t} \tag{3}$$

$$\frac{Q_1}{a_1}=\frac{Q_1}{\sqrt{\gamma g R T_1}}=\frac{1}{\sqrt{\gamma g R t_{s1}}}\frac{Q_1}{\sqrt{\theta}} \tag{4}$$

$$\frac{Q_1}{a_1}=\frac{W_a R T_1}{P_1\sqrt{\gamma g R T_1}}=\frac{\sqrt{R t_{s1}}}{p_{s1}\sqrt{\gamma g}}\frac{W_a\sqrt{\theta}}{\delta} \tag{5}$$

The leaving air angle β_3 from the guide vanes may be either determined from direct tests on the guide vanes or estimated from design data or from cascade tests on similar vanes. (See reference 15.) If the value of β_3 is known for one guide-vane setting ψ, its value β_3' for any other unstalled setting ψ' can be determined with sufficient accuracy by the empirical relation based on airfoil-cascade tests (references 12 and 13)

$$\beta_3-\beta_3'=K(\psi-\psi') \tag{6}$$

where K is a constant (depending on the solidity) between 0.9 and 1.0.

The value of Q_3/a_1 is then determined from the following implicit equation (derived in appendix A as equation (38)):

$$\frac{Q_1}{a_1 A_3\cos\beta_3}=\frac{Q_3}{a_1 A_3\cos\beta_3}\left[1-\left(\frac{\gamma-1}{2}\right)\left(\frac{Q_3}{a_1 A_3\cos\beta_3}\right)^2\right]^{\frac{1}{m'-1}} \tag{7}$$

where m' is the polytropic exponent, which is related to the polytropic expansion efficiency by

$$\frac{m'-1}{m'}=\frac{\gamma-1}{\gamma}\eta_p' \tag{8}$$

The solution of equation (7) based on $\eta_p'=0.90$ is shown in figure 5 with Q_1/Q_3 plotted against $Q_1/(a_1A_3\cos\beta_3)$. The value of V_3/a_1 is given by

$$\frac{V_3}{a_1}=\left(\frac{Q_1}{a_1 A_3\cos\beta_3}\right)\left(\frac{Q_3}{Q_1}\right) \tag{9}$$

and the axial component and the whirl component are determined from

$$\frac{v_3}{a_1}=\frac{V_3}{a_1}\cos\beta_3=\frac{Q_3}{a_1 A_3} \tag{10}$$

and

$$\frac{V_{w,3}}{a_1}=\frac{V_3}{a_1}\sin\beta_3 \tag{11}$$

The density ratio across the guide vanes is obtained from the continuity relation

$$\frac{\rho_3}{\rho_1}=\frac{Q_1}{Q_3} \tag{12}$$

and pressure ratio, temperature ratio, and velocity-of-sound ratio are obtained from the polytropic relations

$$\frac{p_3}{p_1}=\left(\frac{\rho_3}{\rho_1}\right)^{m'}=\left(\frac{t_3}{t_1}\right)^{\frac{m'}{m'-1}}=\left(\frac{a_3}{a_1}\right)^{\frac{2m'}{m'-1}} \tag{13}$$

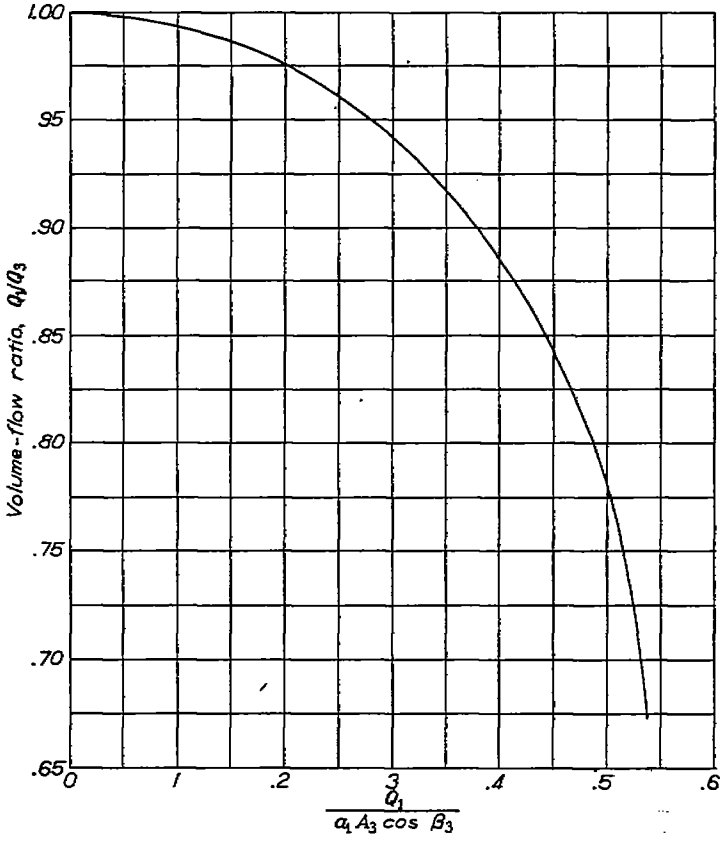

FIGURE 5.—Determination of volume flow preceding first rotor row. η_p', 0.90.

For convenience of calculation, these four ratios are plotted in figure 6 as functions of the variable $Q_1/(a_1A_3\cos\beta_3)$ for $\eta_p'=0.90$.

The relative whirl component of air velocity can now be obtained from

$$\frac{W_{w,3}}{a_1}=\frac{U_3}{a_1}-\frac{V_{w,3}}{a_1} \tag{14}$$

The relative air angle and the resultant relative air velocity ahead of the first row of rotor blades can be readily calculated from the two velocity components if the small radial component of velocity is neglected.

Calculation for typical stage.—The calculation procedure for the first row of rotor blades is essentially the same as that used in a typical stage and need not be separately presented. The special conditions encountered in the first row of rotor blades will be discussed after the general method for a typical stage is presented. A velocity diagram for a typical stage is

shown in figure 7. The air enters the stator row of blades with a velocity V_t at an angle β_t with respect to the compressor axis. The air in passing through the stator blades is deflected through an angle $\beta_t - \beta_{t+1}$ and leaves the blades with a velocity V_{t+1} at an angle β_{t+1}.

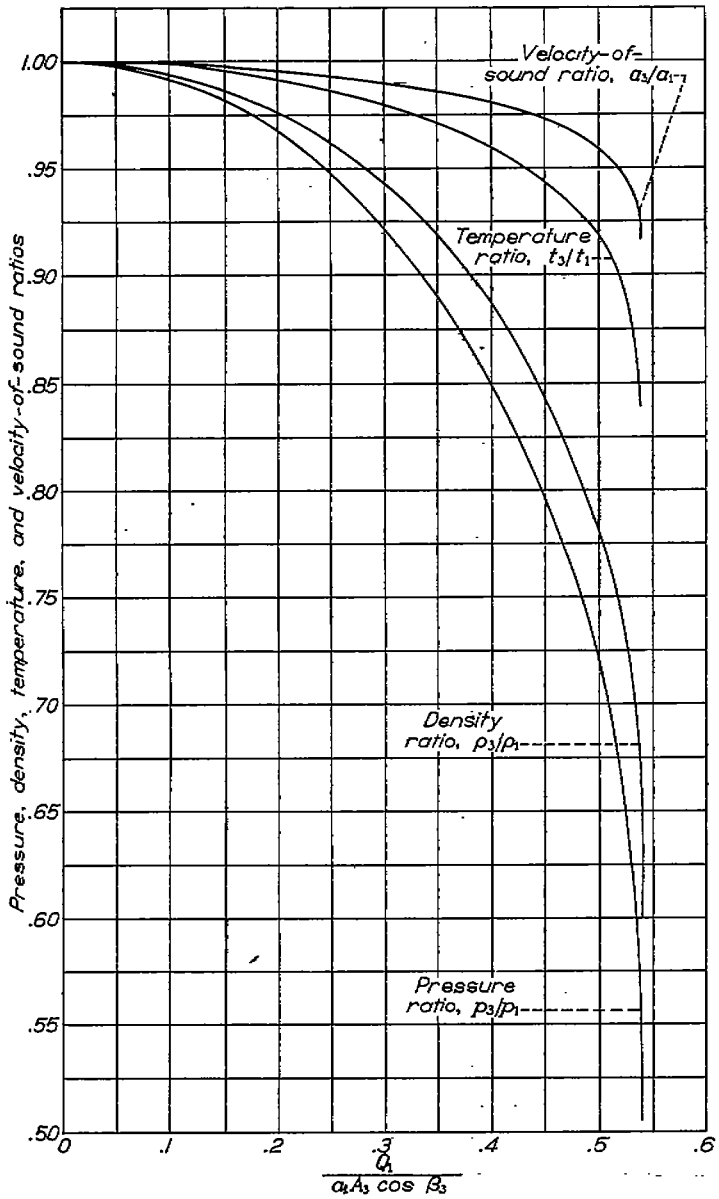

FIGURE 6.—Determination of pressure ratio, density ratio, temperature ratio, and velocity-of-sound ratio over entrance guide vanes. η_p', 0.90.

The air enters the following row of rotor blades with a velocity relative to the rotor of W_{t+1} at an angle ϕ_{t+1} with respect to the compressor axis and leaves the rotor row with a velocity W_{t+2} at an angle ϕ_{t+2}. The axial component of air velocity v is shown increasing from station to station, as is the case in the NACA eight-stage axial-flow compressor. The value of U also may be slightly changed from station to station because of the change in mean radius.

In order to obtain the conditions at the exit of a row of blades from the conditions at the entrance to the row, it is necessary to know the angle through which the air is turned while passing through the blades. Cascade tests (reference 12) have indicated that, for solidities in the neighborhood of

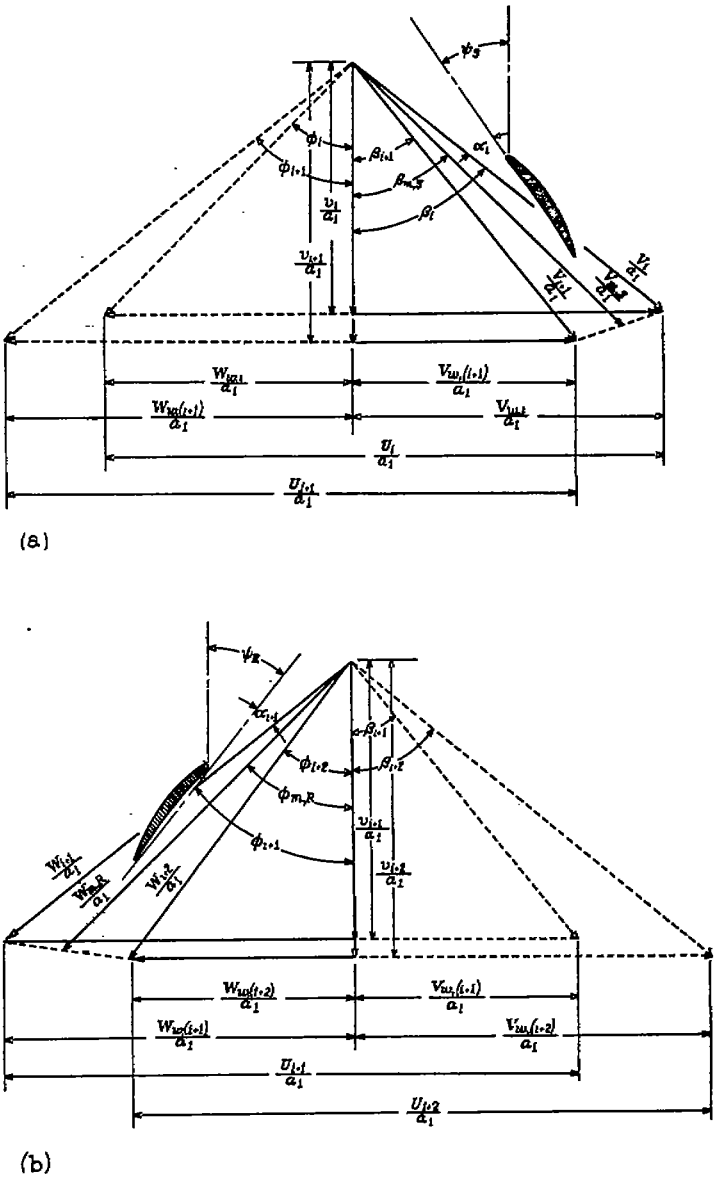

(a) Stator.
(b) Rotor.

FIGURE 7.—Velocity diagram for typical stage of axial-flow compressor.

unity, a good approximation to the turning angle is given by the empirical rule

$$\beta_t - \beta_{t+1} = K(\alpha_t - \alpha_0) \tag{15}$$

where K is a constant slightly less than 1 and α_0 is the angle of attack at zero lift for the given blade section as an isolated airfoil. For a solidity of unity, a value of K of 0.9 was found

to be satisfactory. Although a value of 0.9 was used with satisfactory results in the resetting of the blades of the NACA eight-stage axial-flow compressor, somewhat greater accuracy might be obtained by taking K as a function of the solidity increasing with an increase in solidity. Other empirical relations for turning angle, of course, may be used in place of equation (15) or, if sufficient cascade data for the blade sections used in the compressor are available, the turning angle may be obtained from these data.

The air angle β_{t+1} leaving the stator row can be expressed in terms of β_t, α_0, and ψ_S (fig. 7) by the use of equation (15) and the relation

$$\alpha_t=\beta_t-\psi_S \tag{16}$$

which gives

$$\beta_{t+1}=(1-K)\,\beta_t+K\psi_S+K\alpha_0 \tag{17}$$

The corresponding relation for the following row of rotor blades is

$$\phi_{t+2}=(1-K)\,\phi_{t+1}+K\psi_R+K\alpha_0 \tag{18}$$

With given stator-blade-angle setting and inlet conditions, the leaving air angle is calculated from equation (17) and the value of v_{t+1}/a_1 is determined by a trial-and-error solution of the following equation (derived in appendix B as equation (50)):

$$\frac{v_t}{a_1}=\frac{v_{t+1}}{a_1}\frac{A_{t+1}}{A_t}\left\{1+\frac{\gamma-1}{2}\left(\frac{a_1}{a_t}\right)^2\left[\frac{(v_t/a_1)^2}{\cos^2\beta_t}-\frac{(v_{t+1}/a_1)^2}{\cos^2\beta_{t+1}}\right]\right\}^{\frac{1}{m-1}} \tag{19}$$

Inasmuch as v_{t+1}/a_1 will be nearly equal to v_t/a_1, a satisfactory approximation can usually be obtained by a few trials. The density ratio ρ_{t+1}/ρ_t is determined in carrying out the foregoing approximations and is equal to the expression in the braces raised to the indicated power in equation (19). The pressure ratio, the temperature ratio, and the velocity-of-sound ratio are determined from the polytropic relations

$$\frac{p_{t+1}}{p_t}=\left(\frac{\rho_{t+1}}{\rho_t}\right)^m=\left(\frac{t_{t+1}}{t_t}\right)^{\frac{m}{m-1}}=\left(\frac{a_{t+1}}{a_t}\right)^{\frac{2m}{m-1}} \tag{20}$$

The value of the exponent m can be determined from the estimated polytropic efficiency of compression by

$$\frac{m}{m-1}=\frac{\gamma}{\gamma-1}\,\eta_p \tag{21}$$

and (unlike the exponent m' for expansion) is greater than γ. The lift coefficient is calculated from the relation

$$C_L=\frac{2\Delta w}{\sigma}\cos\beta_m=\frac{2}{\sigma}(\tan\beta_t-\tan\beta_{t+1})\cos\beta_m \tag{22}$$

where

$$\tan\beta_m=\frac{\tan\beta_t+\tan\beta_{t+1}}{2} \tag{23}$$

(See reference 1.) Equation (23) neglects variations of axial velocity and effect of drag but, because of uncertainties regarding the most desirable lift coefficient, is considered adequate.

The calculation procedure for the following row of rotor blades is essentially the same as for the stator blades. The inlet conditions relative to the rotor are determined from the conditions leaving the stator row, and the relative air angle ϕ_{t+2} leaving the rotor row is determined from equation (18). The value of v_{t+2}/a_1 is then determined from the equation (derived in appendix B as equation (51))

$$\frac{v_{t+1}}{a_1}=\frac{v_{t+2}}{a_1}\frac{A_{t+2}}{A_{t+1}}\left\{1+\frac{\gamma-1}{2}\left(\frac{a_1}{a_{t+1}}\right)^2\left[\frac{(v_{t+1}/a_1)^2}{\cos^2\phi_{t+1}}-\frac{(v_{t+2}/a_1)^2}{\cos^2\phi_{t+2}}+X\right]\right\}^{\frac{1}{m-1}} \tag{24}$$

where

$$X=\left(\frac{U_{t+2}}{a_1}\right)^2-\left(\frac{U_{t+1}}{a_1}\right)^2$$

and the lift coefficient calculated from the equations analogous to equations (22) and (23), with the air angles relative to the rotor replacing those relative to the stator.

Special conditions for first row of rotor blades.—When only the stator blades are reset, conditions are somewhat different for the first row of rotor blades than for a typical stage, because, as has already been pointed out, it is not practical to control the lift coefficients on the first row of rotor blades to an appreciable extent by the adjustment of the entrance guide vanes. Consequently, when the stator blades are reset for a load coefficient considerably below the design value, the first row of rotor blades will be stalled and the method presented herein will not be accurate for that row of blades. The actual turning angle and density rise will be less and the axial velocity leaving the blades, higher than calculated. At a somewhat lower inlet-air flow, however, the axial velocity and the air angle leaving the following row of stator blades (station 5, fig. 1), and hence the flow conditions in the subsequent stages, should be substantially correct as calculated. Somewhat higher accuracy, of course, could be obtained by basing the turning angle and the density rise for the first row of rotor blades on cascade tests under similar stalled conditions.

APPLICATION OF BLADE-RESETTING CALCULATIONS TO NACA EIGHT-STAGE AXIAL-FLOW COMPRESSOR

Calculations of guide-vane and stator-blade settings of the NACA eight-stage axial-flow compressor for 75 percent of design speed over a series of load coefficients ranging from 0.28 to 0.70 are summarized in table II. The blade resettings were calculated for load coefficients appreciably less than the design value of 0.64 because computations indicated that, for certain practical gas-turbine applications, the compressor would be operating at appreciably reduced load coefficients at speeds below the design.

The following values of constants were assumed in these calculations:

Adiabatic exponent (for normal air), γ	1.3947
Polytropic exponent for compression (corresponding to $\eta_p=0.85$), m	1.5000
Polytropic exponent for expansion (corresponding to $\eta_p'=0.90$), m'	1.3417
Turning-angle constant, K:	
For entrance guide vanes	1.0
For all other blade rows	0.9

The changes of blade angles from the design settings are very large in some cases, amounting to approximately 36° for the first four stator rows at the lowest load coefficient calculated. (See table II at a load coefficient of 0.28.) Changes required are fairly large for all resettings (over 20° for some of the rows) because the speed for which the blades were reset was appreciably below the design speed.

The most favorable flow conditions at the compressor inlet were obtained for the blade resettings for high load coefficients. At the lower load coefficients, the angles of attack and the "theoretical" lift coefficients were excessively high on the first row of rotor blades, which should result in stalling of these blades. Different entrance-guide-vane settings were tried but the improvement was found to be small (table I), especially at the tips of the rotor blades. The most desirable entrance-guide-vane setting under these conditions is very uncertain. Because of increased losses in the entrance guide vanes resulting from large increases in guide-vane angles, the increase over design setting was limited to 20°. This large increase in guide-vane angle was used only for a load coefficient of 0.48 because the improvement in rotor-blade conditions at lower load coefficients appeared to be so slight that increasing the guide-vane losses by large changes in the guide-vane settings was hardly warranted.

Not only is the angle of attack on the first row of rotor blades excessively high for blade resettings for low load coefficients but the relative Mach number at the entrance to these blades increases as the load coefficient decreases because of the small whirl component of velocity produced by the entrance guide vanes. Inasmuch as the critical Mach number is very low for high angles of attack, large compression-shock losses may also occur at the low load coefficients even when the compressor is operating at 75 percent of design speed. Because of the uncertainty regarding the losses through the first row of rotor blades, it is difficult to estimate the over-all performance that might be expected from the compressor with the stator blades reset for very low load coefficients.

The maximum practicable load coefficients for resetting stator blades appear to be determined principally by the relative Mach number on the last row of rotor blades. At a load coefficient of 0.70 (table II), the relative Mach number at the entrance to the last rotor is 0.83, which is appreciably above the critical Mach number for these blades even for the low lift coefficient of 0.50.

TEST OF THEORY OF STATOR-BLADE RESETTING

The effect on the performance of an axial-flow compressor of resetting the stator blades according to the theory presented was determined by comparing the performance of the NACA eight-stage axial-flow compressor with design blade setting and with the stator blades reset for 75 percent of design speed for load coefficients of 0.48 and 0.65. The design theory, the theory of operation, and the complete details of construction of the NACA eight-stage axial-flow compressor (fig. 8) are given in reference 1 and modifications of the original blading (fig. 9), as well as descriptions of the setup and instrumentation (fig. 2), as used in the present investigation are given in reference 16. The compressor was investigated over a range of compressor Mach numbers from 0.2 to 0.8; the design Mach number of 0.968 was therefore not reached in the present tests. Because of limitations of power and outlet-air temperature at high speeds, most of the tests were run with an inlet-air pressure of 10.16 inches of mercury absolute (corresponding to a pressure altitude of 27,000 ft) and an inlet-air temperature of 0° F. At Mach numbers of 0.2 and 0.3 with design blade-angle settings, it was impossible to throttle the inlet air to the desired pressure and still cover the normal flow range of the compressor because of imperfect fitting of the inlet throttle. These tests were therefore conducted at somewhat higher inlet-air pressures corresponding to altitudes ranging from 1000 to 10,000 feet. The inlet throttle was modified when the stator blades were reset in order that the subsequent tests could be run at the selected inlet pressure. In order to determine the effect of inlet-air conditions at low speeds, the tests at a compressor Mach number of 0.2 with the first blade resetting (load coefficient, 0.48) were repeated with standard sea-level inlet-air conditions of 29.92 inches of mercury absolute and 59° F.

At the high speeds, the flow ranges for each compressor Mach number were selected by starting with a low pressure ratio and progressively decreasing the flow until a definite surge occurred. At a compressor Mach number of 0.8, however, the compressor was not surged except for the first blade resetting (load coefficient, 0.48) because of power limitation. At the lower compressor speeds, where no

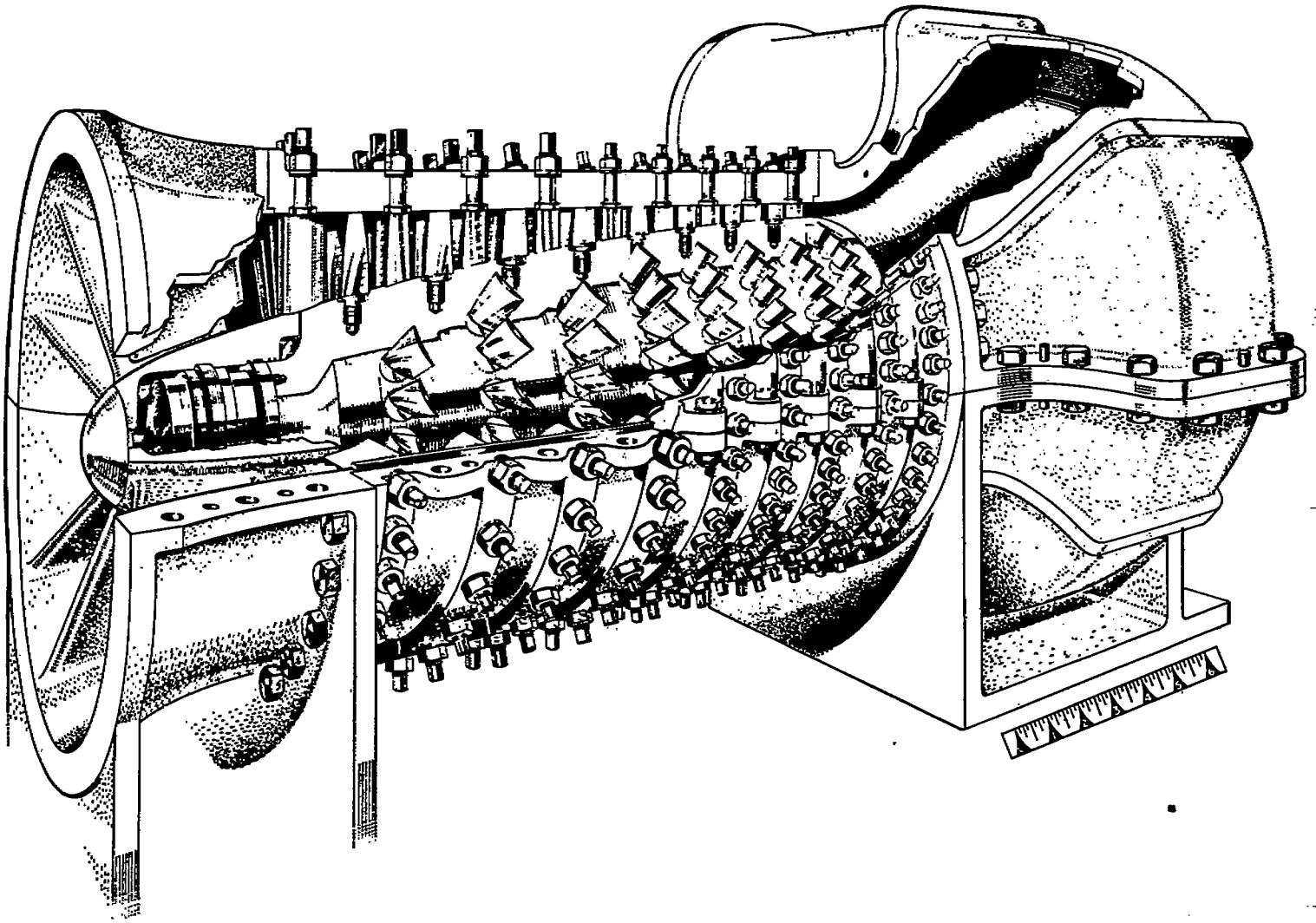

FIGURE 8.—NACA eight-stage axial-flow compressor

definite surging occurred, the flow was decreased as far as possible by closing the inlet throttle.

Effect of stator-blade resettings on performance characteristics.—Performance characteristics of the compressor for the design blade settings are shown in figure 10 and those with the stator blades reset for 75 percent of design speed and for the coefficients of 0.48 and 0.65 are shown in figures 11 and 12, respectively. These performance results are based upon total-pressure and total-temperature rise between the inlet tank and the outlet duct. The characteristics for the different blade settings are compared in figures 13 and 14. Results for the design blade setting are not shown for compressor Mach numbers of 0.2 and 0.3 (fig. 13) because these tests were not run with the same inlet-air conditions as for the two resettings. Figure 15 presents comparisons of the peak adiabatic temperature-rise efficiencies, the peak pressure ratios, and load coefficients at the peak-efficiency points for the three blade settings as a function of the compressor Mach number.

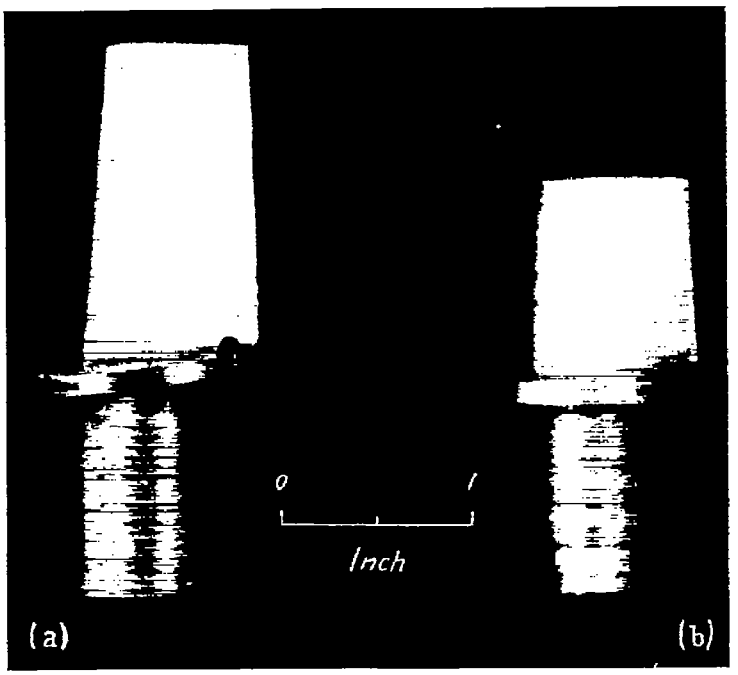

(a) First rows. (b) Last rows.

FIGURE 9.—Construction of modified rotor blades.

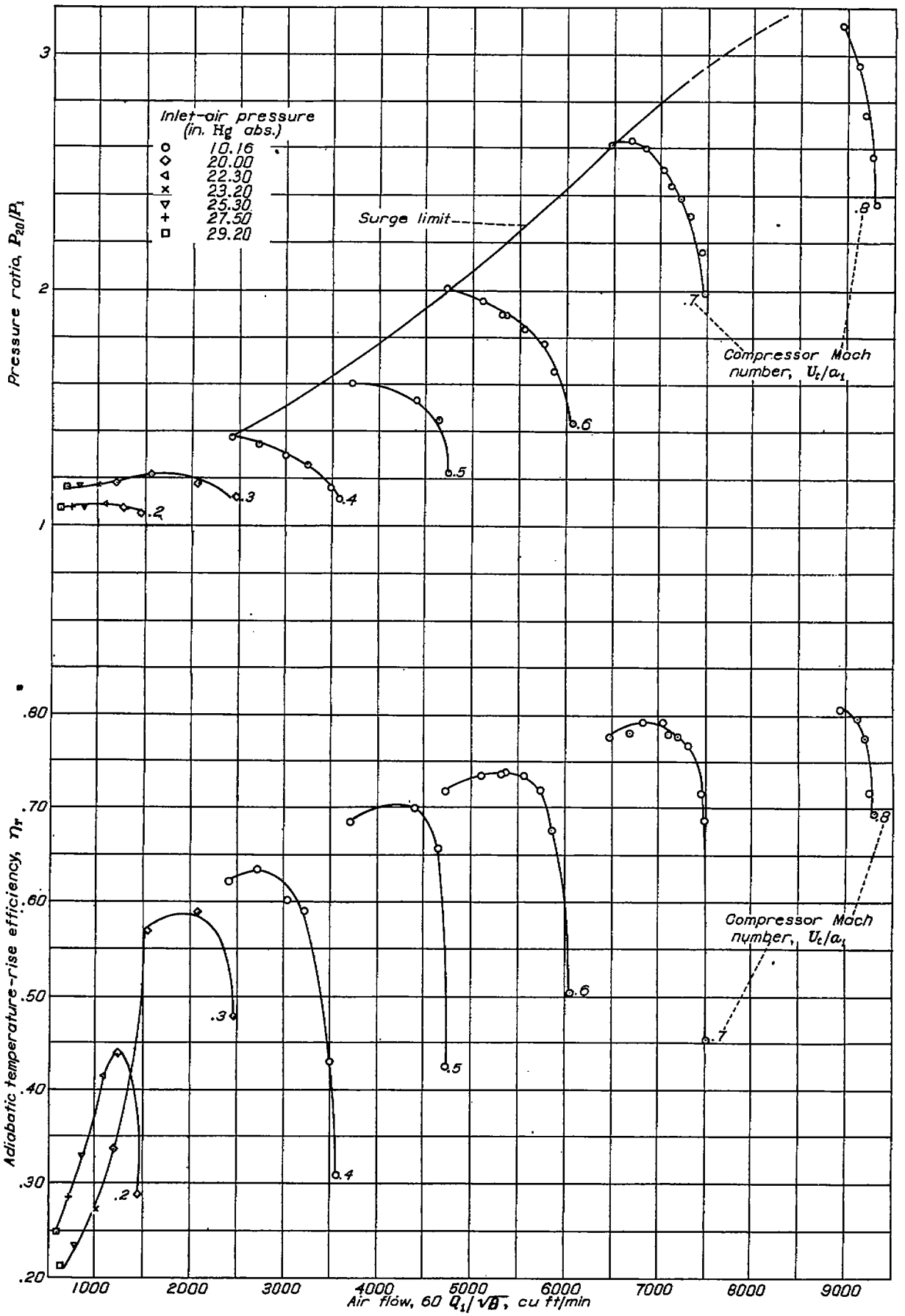

FIGURE 10.—Performance characteristics of axial-flow compressor with design blade angles at inlet-air temperature of 0° F.

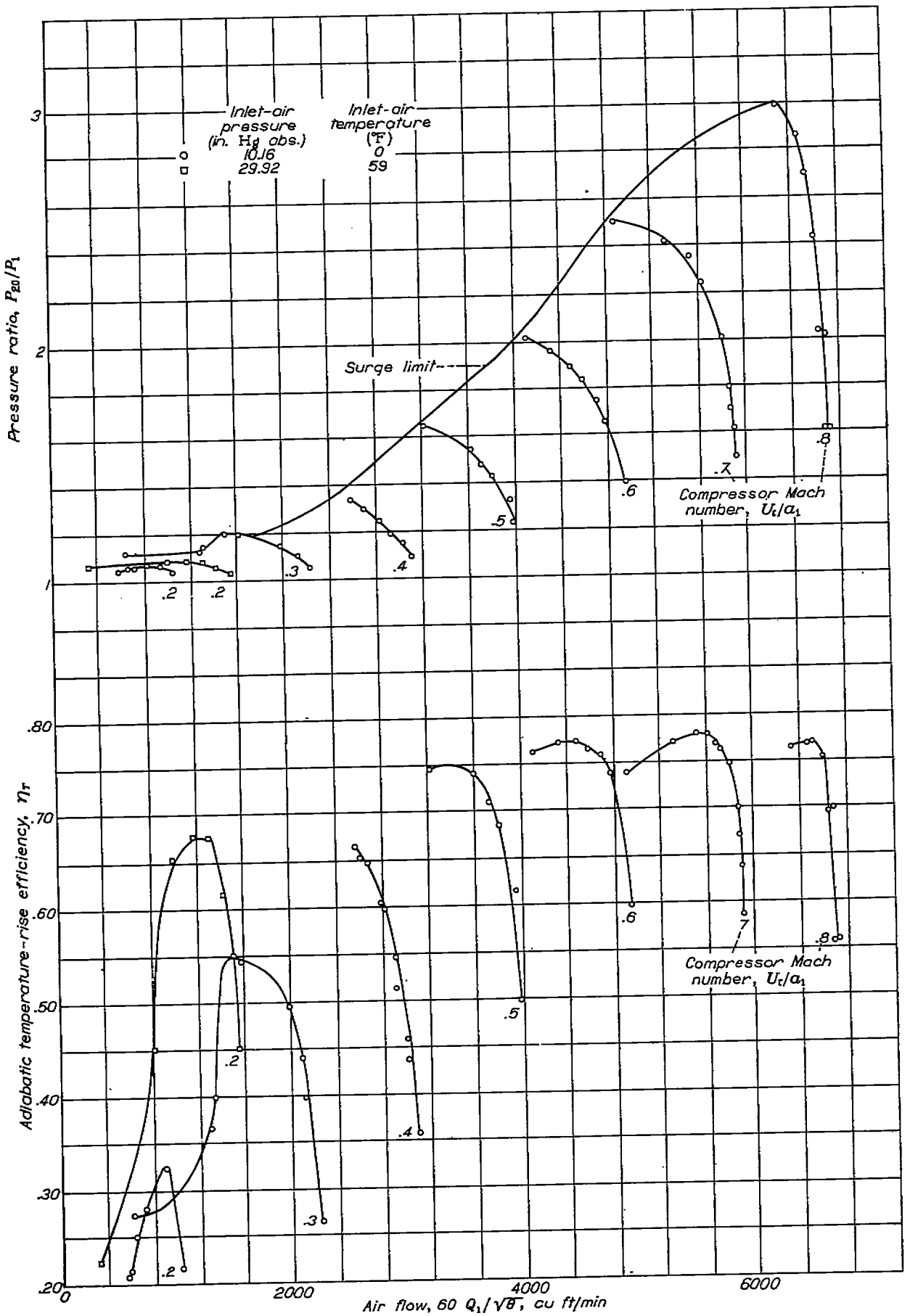

FIGURE 11.—Performance characteristics of axial-flow compressor with stator blades reset for 75 percent of design speed and load coefficient of 0.42.

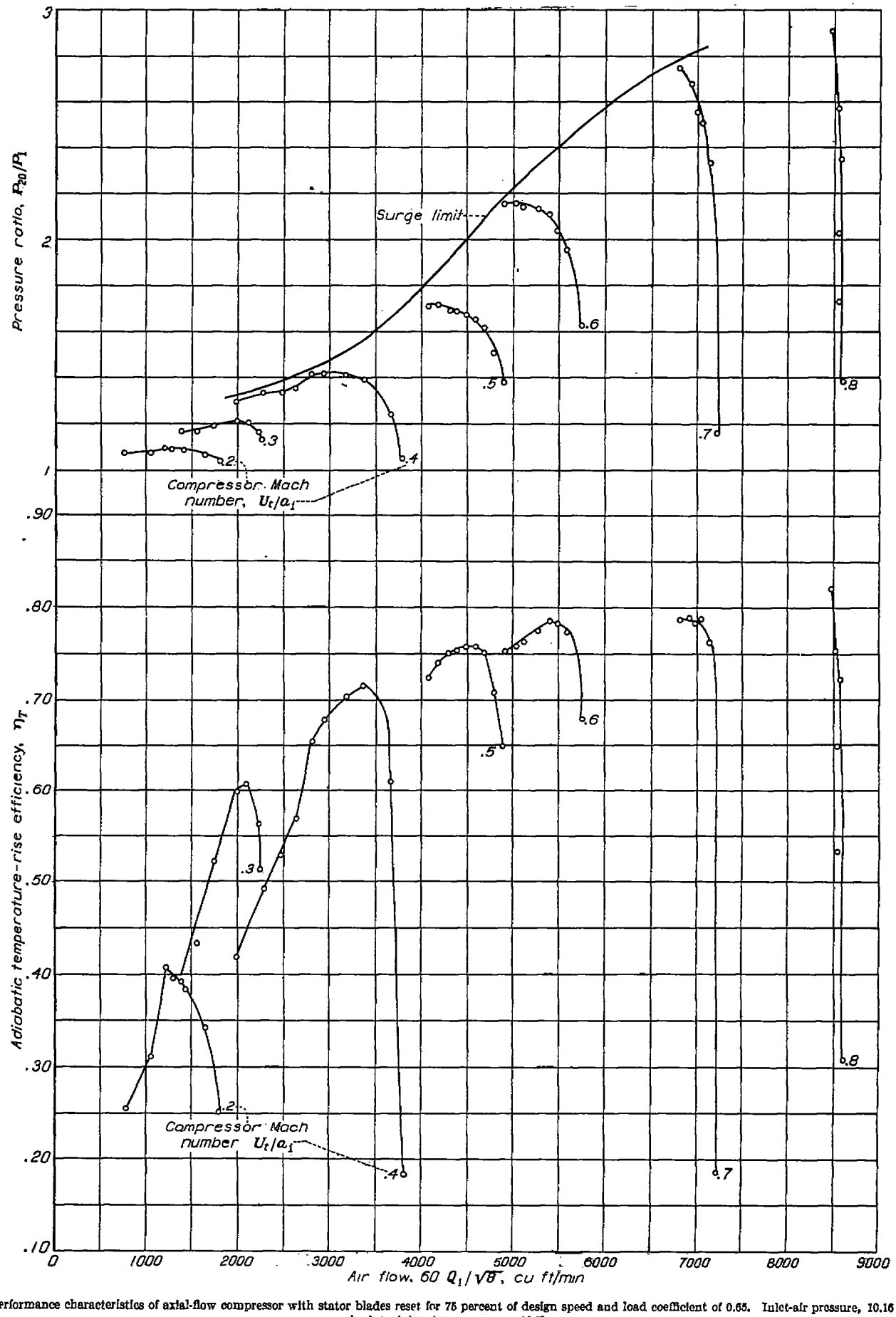

FIGURE 12.—Performance characteristics of axial-flow compressor with stator blades reset for 75 percent of design speed and load coefficient of 0.65. Inlet-air pressure, 10.16 inches mercury absolute; inlet-air temperature, 0° F.

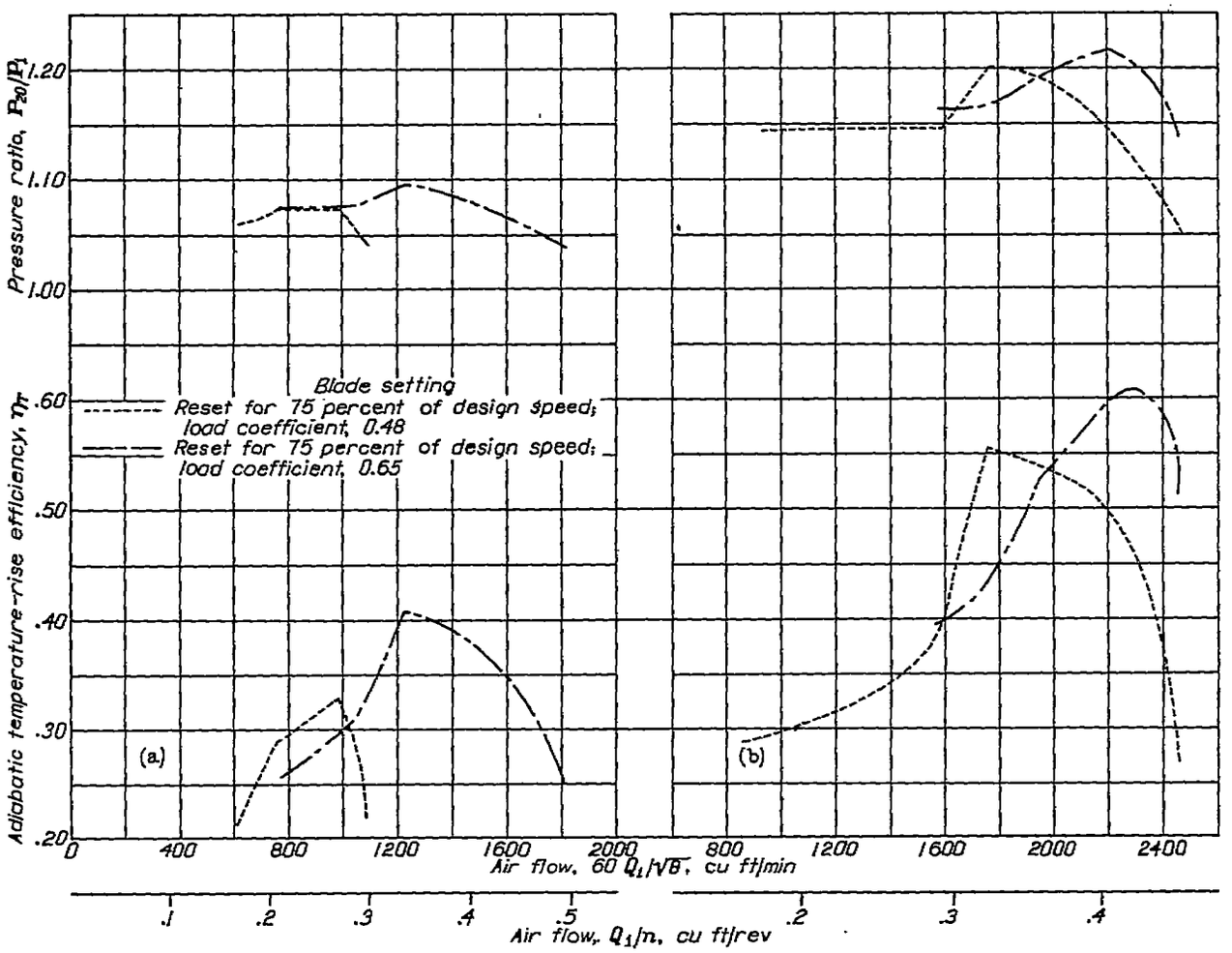

(a) Compressor Mach number, 0.2.

(b) Compressor Mach number, 0.8.

FIGURE 13.—Comparison of performance characteristics of axial-flow compressor with stator blades reset for 75 percent of design speed at load coefficients of 0.48 and 0.65.

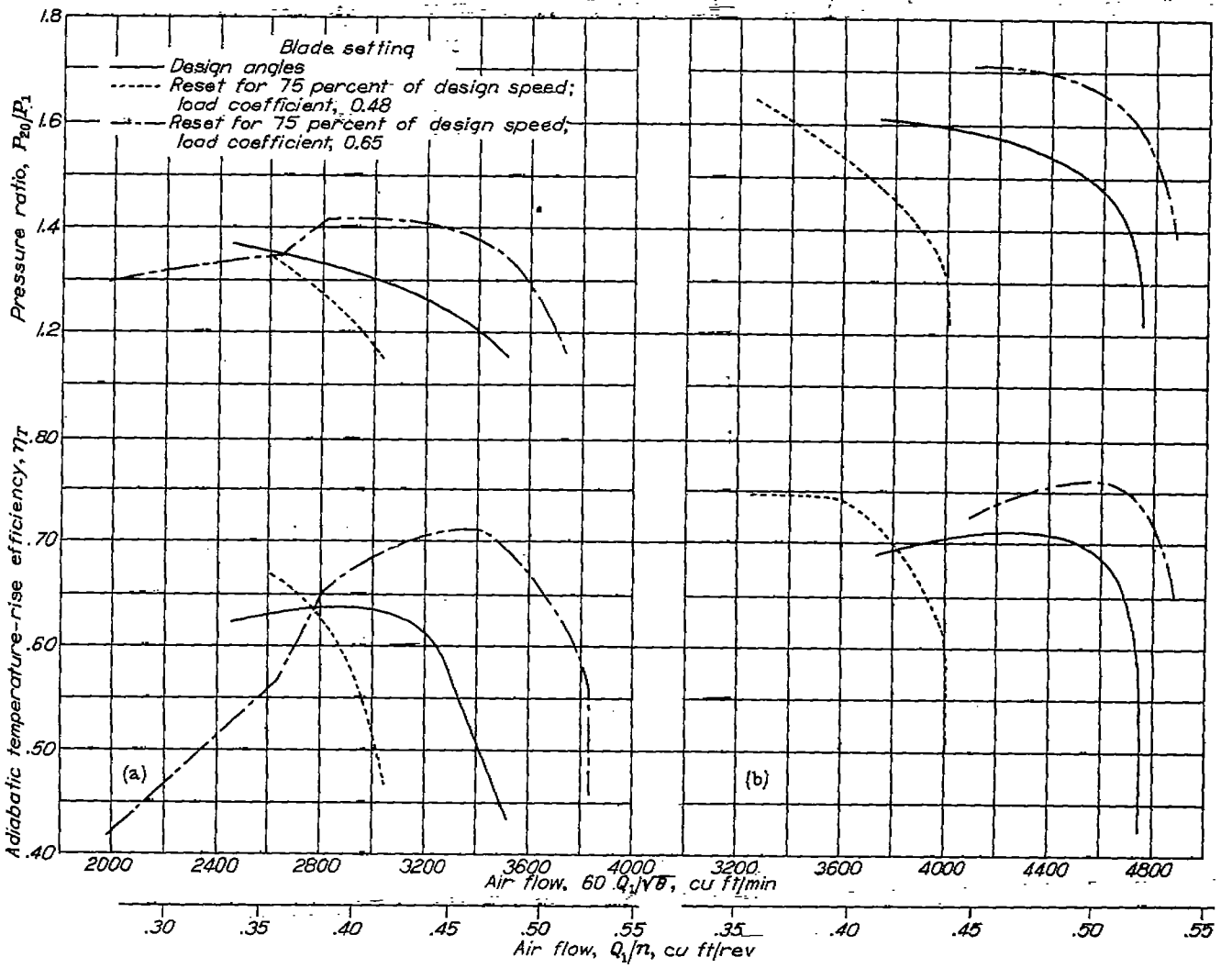

(a) Compressor Mach number, 0.4

(b) Compressor Mach number, 0.8.

FIGURE 14.—Comparison of performance characteristics of axial-flow compressor with design blade setting and with stator blades reset for 75 percent of design speed at load coefficients of 0.4 and 0.65.

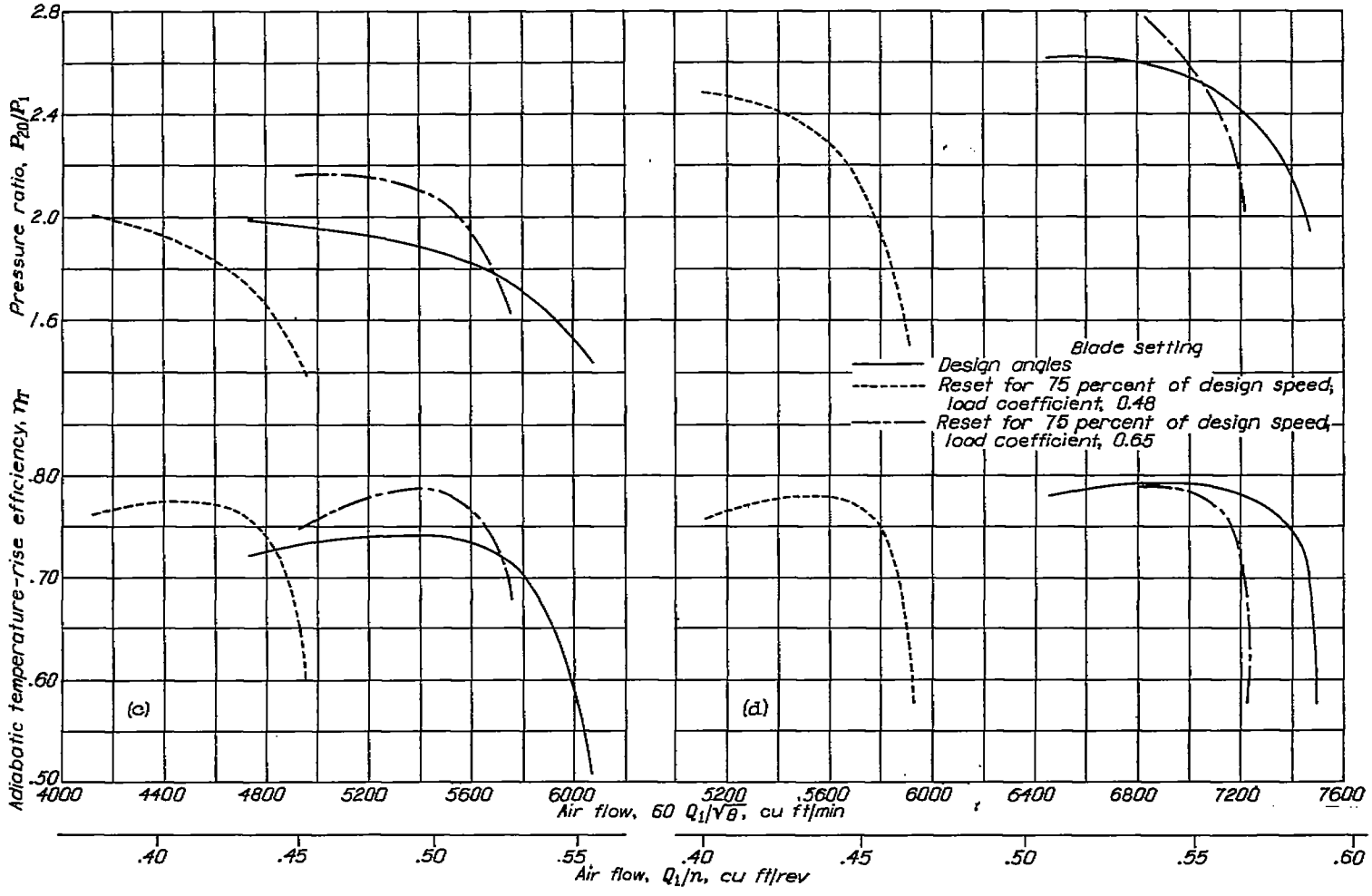

(c) Compressor Mach number, 0.6.

(d) Compressor Mach number, 0.7.

FIGURE 14.—Continued. Comparison of performance characteristics of axial-flow compressor with design blade setting and with stator blades reset for 75 percent of design speed at load coefficients of 0.48 and 0.65.

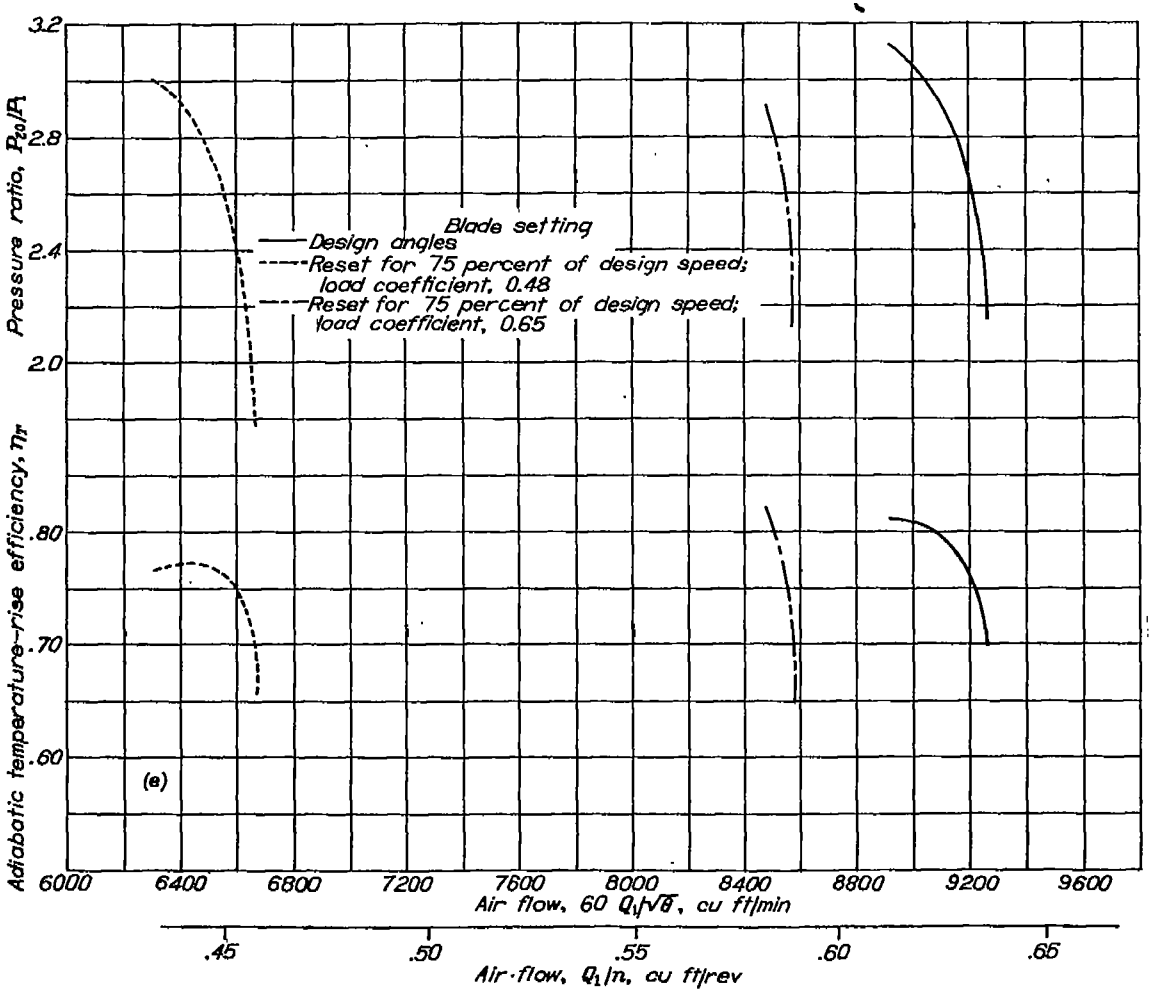

(e) Compressor Mach number, 0.8.

FIGURE 14.—Concluded. Comparison of performance characteristics of axial-flow compressor with design blade setting and with stator blades reset for 75 percent of design speed at load coefficients of 0.48 and 0.65.

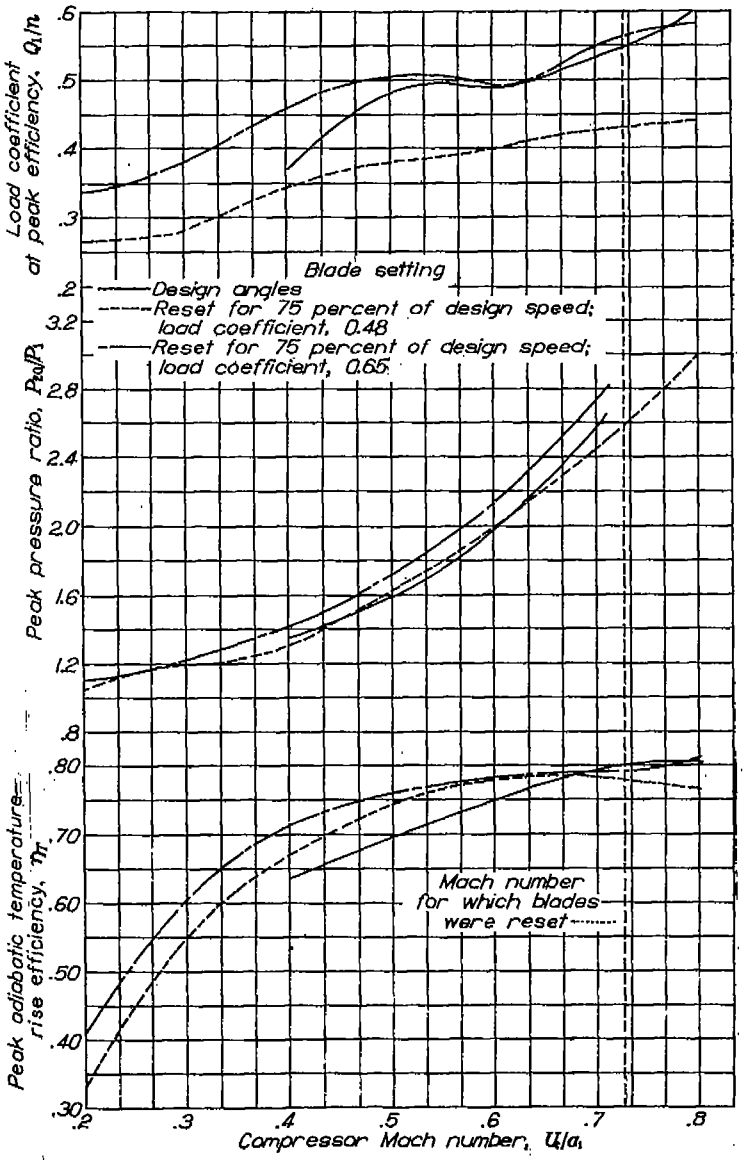

FIGURE 15.—Peak-performance characteristics of axial-flow compressor with blades set at design angles and with stator blades reset for 75 percent of design speed and load coefficients of 0.48 and 0.65.

For both stator-blade resettings, appreciable increases in peak efficiencies were obtained over those with design angles at compressor Mach numbers below that for which the blades were reset (figs. 14 and 15) and the peak-efficiency curves are much flatter over the range of Mach numbers from 0.4 to 0.8. This shift of the high-efficiency range to lower compressor Mach numbers was expected because the blades were reset for 75 percent of the design compressor Mach number. At the Mach number for which the blades were reset, however, the three different blade settings gave about the same efficiency. At this compressor speed, the slight gain that might have been expected from somewhat more favorable lift coefficients was counteracted by other unfavorable factors such as: (1) rather large deviations from a symmetrical velocity diagram (table II); (2) increase in blade-tip clearances (fig. 16) and poor fairing of the blade bases with the casing resulting from changes of blade setting; (3) necessity of using lift coefficients appreciably below the optimum on a row of stator blades to prevent stalling of the following row of rotor blades (or vice versa); and (4) poor flow conditions for the entrance guide vanes and first row of rotor blades for the low-load-coefficient resetting.

The stator-blade resetting for high load coefficient gave higher peak efficiencies and pressure ratios at all compressor Mach numbers than the resetting for the low load coefficient. The somewhat poorer performance with the resetting for low load coefficient is probably due principally to factors (2) and (4). The increases in tip clearances were much greater for the low-load-coefficient blade resetting because the principal changes in blade settings were made on the inlet stages where the taper of the rotor is large. The lift coefficient on the entrance guide vanes and the distribution of lift on the first row of rotor blades were also less favorable for the low-load-coefficient resetting.

The peak pressure ratios for the stator-blade resetting for a load coefficient of 0.65 are appreciably higher than those for the design blade settings; whereas, for the resetting for a load coefficient of 0.48, the peak pressure ratios are substantially the same as for the design setting over most of the Mach number range. At a compressor Mach number of 0.8, peak pressure ratios were not reached with the design blade setting and with the resetting for a load coefficient of 0.65 because of power limitations.

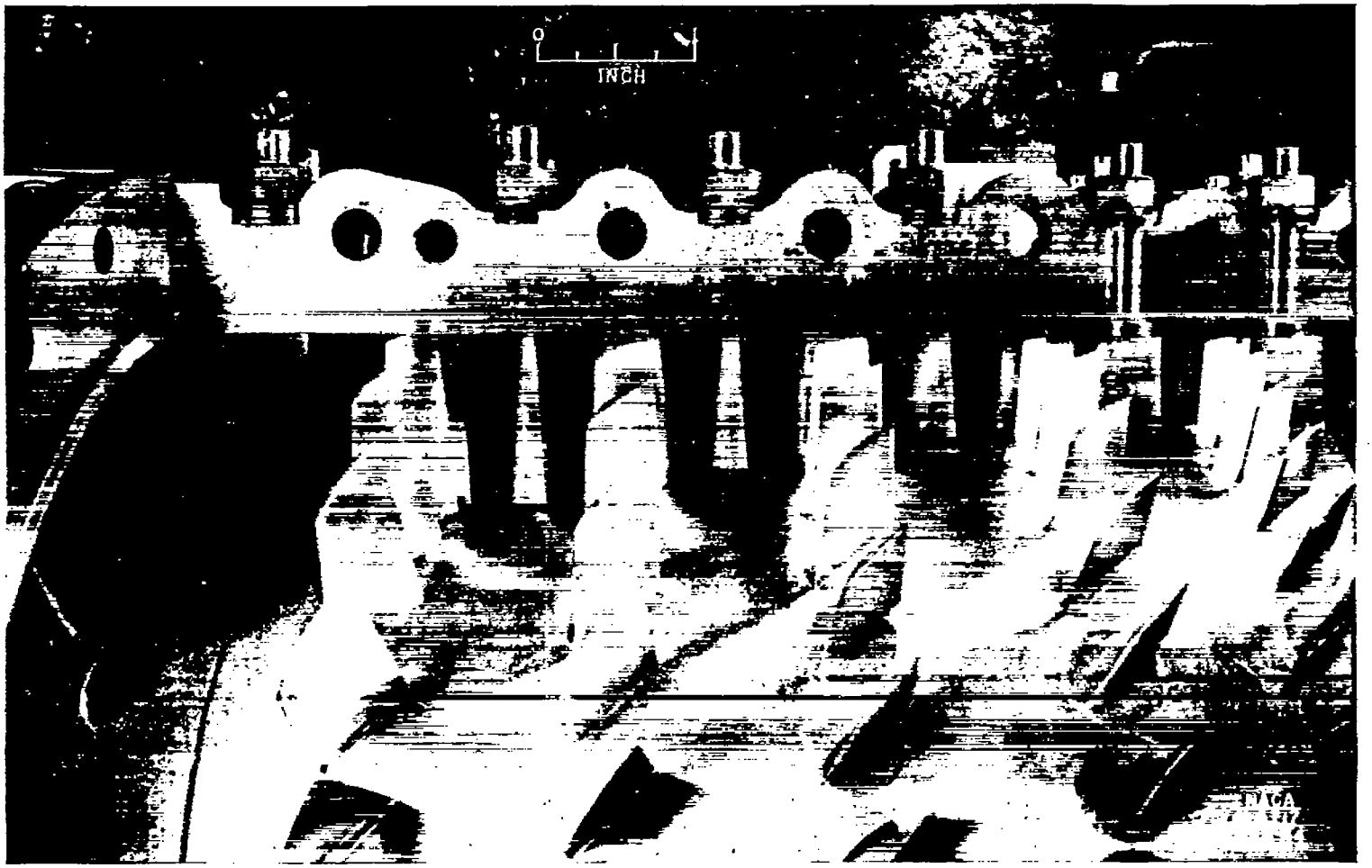

FIGURE 16.—Close-up of rotor of NACA eight-stage axial-flow compressor showing effect of blade-angle changes on clearances at tips of stator blades. Clearances increased at trailing edges, decreased at leading edges.

The tests with the two stator-blade resettings also show that a substantial change in the peak-efficiency flow at a given speed can be obtained by changing the stator-blade settings. With the stator-blade resetting for high load coefficient, the peak-efficiency flows were about 20 to 30 percent greater over the range of Mach numbers tested than with the resetting for low load coefficient. For both stator-blade resettings, the load coefficient obtained at the compressor Mach number for which the blades had been reset was lower than calculated. The differences may be attributed to several assumptions made in the calculation, especially

the neglect of retardation of flow along the passage walls because of surface friction and blade-end losses. The experimental results indicate that the calculated flow should be multiplied by a flow coefficient between 0.85 and 0.90 to obtain the actual flow.

Surging characteristics.—The surging characteristics of the compressor for the three blade settings were investigated for most of the Mach numbers by decreasing the flow as far as possible by closing the throttles. At a Mach number of 0.8 with design angle settings and with the second resetting, a power limitation was encountered and the surge point could not be reached. At the high Mach numbers, the surge limit was not established so accurately as at the low Mach numbers because the compressor might be damaged by surging.

Definite surging was obtained at compressor Mach numbers from 0.4 to 0.7 with the design settings, at Mach numbers from 0.5 to 0.8 for the first stator-blade resettings, and at Mach numbers from 0.5 to 0.7 for the second stator-blade resettings. No definite surging was observed in any of the tests at lower Mach numbers. Instead, as the flow was decreased, a point was reached at which a sudden transition to a lower pressure ratio occurred. (See fig. 17.) Further decrease in flow produced scarcely any change in pressure ratio but a substantial decrease in adiabatic temperature-rise efficiency. Data were not taken below the transition point at a compressor Mach number of 0.4 with the stator blades reset for a load coefficient of 0.48.

The transition phenomenon is probably the result of stalling of one or more rows of blades. It is not quite clear why the sudden drop in pressure with a decrease in flow does not produce surging. The unstable range of flow may be so small that it is difficult to detect. Surging under these conditions might depend on the characteristics of the air supply and the exhaust system and, in particular, on the exhaust suction applied downstream of the outlet throttle. In order to test this hypothesis, exhaust pressures from approximately sea level to about 8 inches of mercury absolute were tried at a compressor Mach number of 0.2 and at sea-level inlet pressure. No noticeable change in the transition point or in the behavior at the transition point was observed.

Effect of inlet-air conditions.—Two tests were run at a compressor Mach number of 0.2 with stator blades reset for a load coefficient of 0.48: one at an inlet-air pressure of 10.16 inches of mercury absolute and an inlet-air temperature of 0° F and the other at approximately standard sea-level inlet-air conditions (29.92 inches of mercury absolute and 59° F). The results (fig. 17) show a very marked effect of inlet conditions on the adiabatic temperature-rise efficiency; a peak efficiency of 32.8 percent was obtained with an inlet-air pressure of 10.16 inches of mercury absolute and a temperature of 0° F, and a peak efficiency of 67.5 percent with standard sea-level inlet-air conditions. This great difference in efficiency is believed to be due to a combination of Reynolds number and heat-transfer effects. Based on the blade-tip velocity U_t, the rotor-blade chord of the first stage c, and the inlet-air density ρ_1 and viscosity μ_1, the value of compressor Reynolds number R_c given by

$$R_c=\frac{\rho_1 U_t c}{\mu_1}$$

was 62,000 for 10.16 inches of mercury absolute and 0° F, and 159,000 for standard sea-level inlet-air conditions. The Reynolds number based on air velocity rather than on blade-tip velocity should be of approximately the same magnitude. For the test with an inlet-air pressure of 10.16 inches of mercury absolute, the Reynolds number is below the critical value of 80,000 to 100,000 given in reference 17; poor performance might therefore be expected.

Heat transfer between the air entering the compressor and the front bearing is also believed to be appreciable because the lubricating oil to the bearing passes through hollow struts of comparatively large area located in the air stream. At times the lubricating oil leaving the bearing was cooler than the oil entering, which indicated that all the heat generated in the bearing by friction and also some heat from the test cell was transferred to the air stream. This heat transfer would have the effect of increasing the temperature rise and lowering the indicated efficiency based on temperature measurements. The air-temperature rise caused by this heat transfer would be greater at the lower inlet pressure

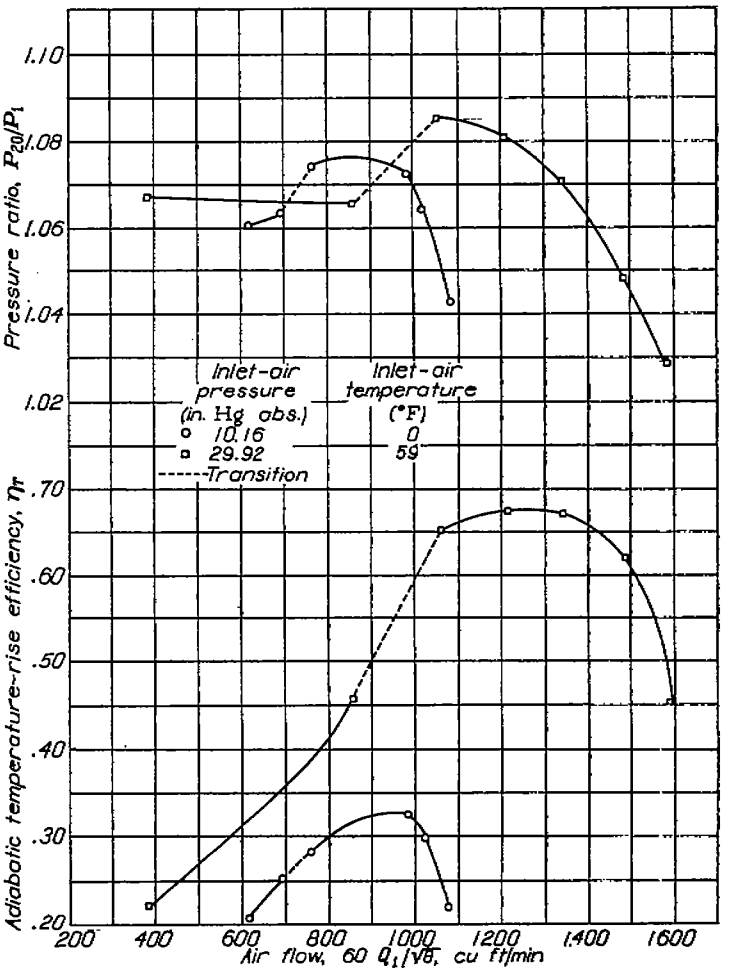

FIGURE 17.—Performance of axial-flow compressor with reset stator blades at compressor Mach number of 0.2 showing effect of inlet-air conditions and range within which transition occurs.

because of the lower air weight flow. The reduction in the temperature-rise efficiency due to this transfer would also be greater at the lower inlet-air temperature because of the larger temperature difference between the oil and the air.

The effect of inlet-air conditions on compressor performance should be much greater at a compressor Mach number of 0.2 than at high Mach numbers for the following reasons: (1) The smaller air weight flow will result in a greater air-temperature rise for a given amount of heat transferred; (2) a given air-temperature rise from heat transfer will produce a greater effect on the adiabatic temperature-rise efficiency because the temperature rise from compression is small; and (3) the Reynolds number effect should be larger because of operation in the critical Reynolds number range and near the stalling point for many of the blades. Unpublished NACA experimental results on both axial-flow and centrifugal compressors indicate that the effect of inlet-air conditions on performance is actually much greater at low than at high compressor Mach numbers.

Pressure distribution through compressor.—Absolute static pressures (figs. 18 to 20) were measured in the depression tank, at the compressor entrance before the guide vanes (CE), at the compressor-casing wall following the entrance guide vanes (GV), following each succeeding row of blades indicated by 1R. 1S, and so forth, in the scroll collector (average of three readings). and in the outlet pipe (average of two readings). The total pressure shown at station 8S is the average of the total-pressure surveys behind the last stator row and the total pressure in the outlet pipe is the average of two readings.

The static-pressure measurements through the compressor were indicative of the relative performance of the different stages of the compressor. A large pressure drop over the last stage, for example, indicates that this stage is acting as a turbine (fig. 18 (c)) and that the air flow is too high for efficient compressor operation. In fact, at the high air flow obtainable by use of altitude exhaust, the last stages acting as turbines could be made to drive the compressor without the aid of the dynamometers. (The compressor was always started by this means.) The total and static pressures after the last stator (station 8S) from figure 18 (c) indicate supersonic velocities. Figures 18 (a) and 18 (b) show appreciably higher pressure rises over the rotor than over the stator rows for the last stages. These results are qualitatively similar to the calculated results (table II) but not quantitatively comparable because of the different reference radii. (The static-pressure measurements were taken at the casing wall, whereas the calculations were made for the mean radius.) The pressure distribution at the high flows is extremely sensitive to changes in flow, as is shown by figures 18(b) and 18(c).

The pressure distribution at peak efficiency for the lower-load-coefficient resetting (fig. 19 (b)) shows a more uniform pressure rise over the rotor and stator blades of the last stages than for the higher-load-coefficient resetting (fig. 18 (b)) in accordance with the calculated pressure ratios (table II). The average pressure ratios per stage obtained at the peak-efficiency flows for both resettings, however, were higher than the calculated values, which indicated that the best over-all efficiencies were obtained at somewhat higher lift coefficients and lower air flows than used in the blade-resetting calculations.

A fairly uniform pressure rise was obtained at the peak-efficiency flow for the lower-load-coefficient blade resetting at a compressor Mach number of 0.2 and standard sea-level inlet-air conditions (fig. 20 (b)) although the flow conditions near the inlet appeared unfavorable. The absence of pressure drop through the entrance guide vanes indicated

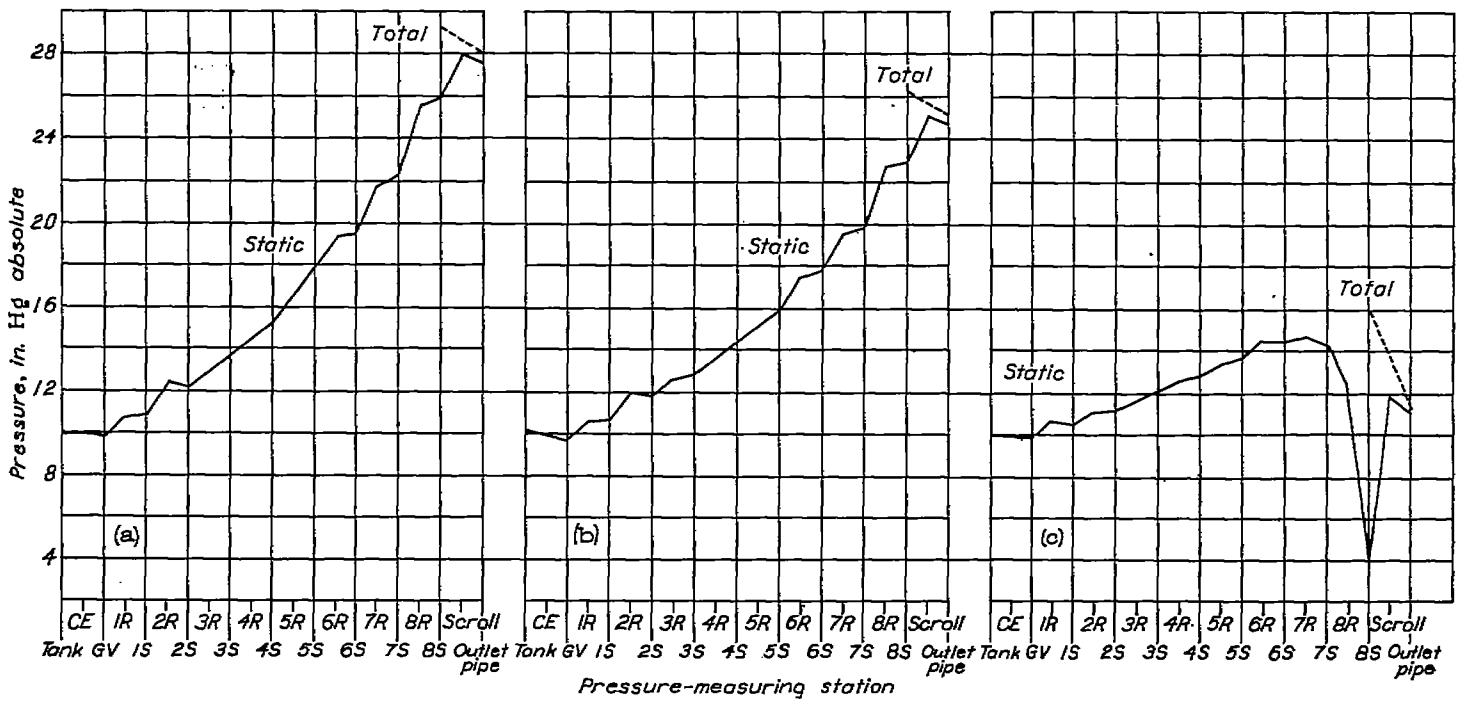

(a) Q_1/n, 0.533; η_T, 0.787. (b) Q_1/n, 0.552; η_T, 0.789. (c) Q_1/n, 0.565; η_T, 0.186.

FIGURE 18.—Pressure distribution from inlet tank to outlet pipe with stator blades reset for 75 percent of design speed at load coefficient of 0.65. Compressor Mach number, 0.7; inlet-air temperature, 0° F; inlet-air pressure, 10.16 inches mercury absolute. Pressure measurements made after each blade row. CE, at compressor entrance; GV, after guide vanes; R, after rotor blades; S, after stator blades.

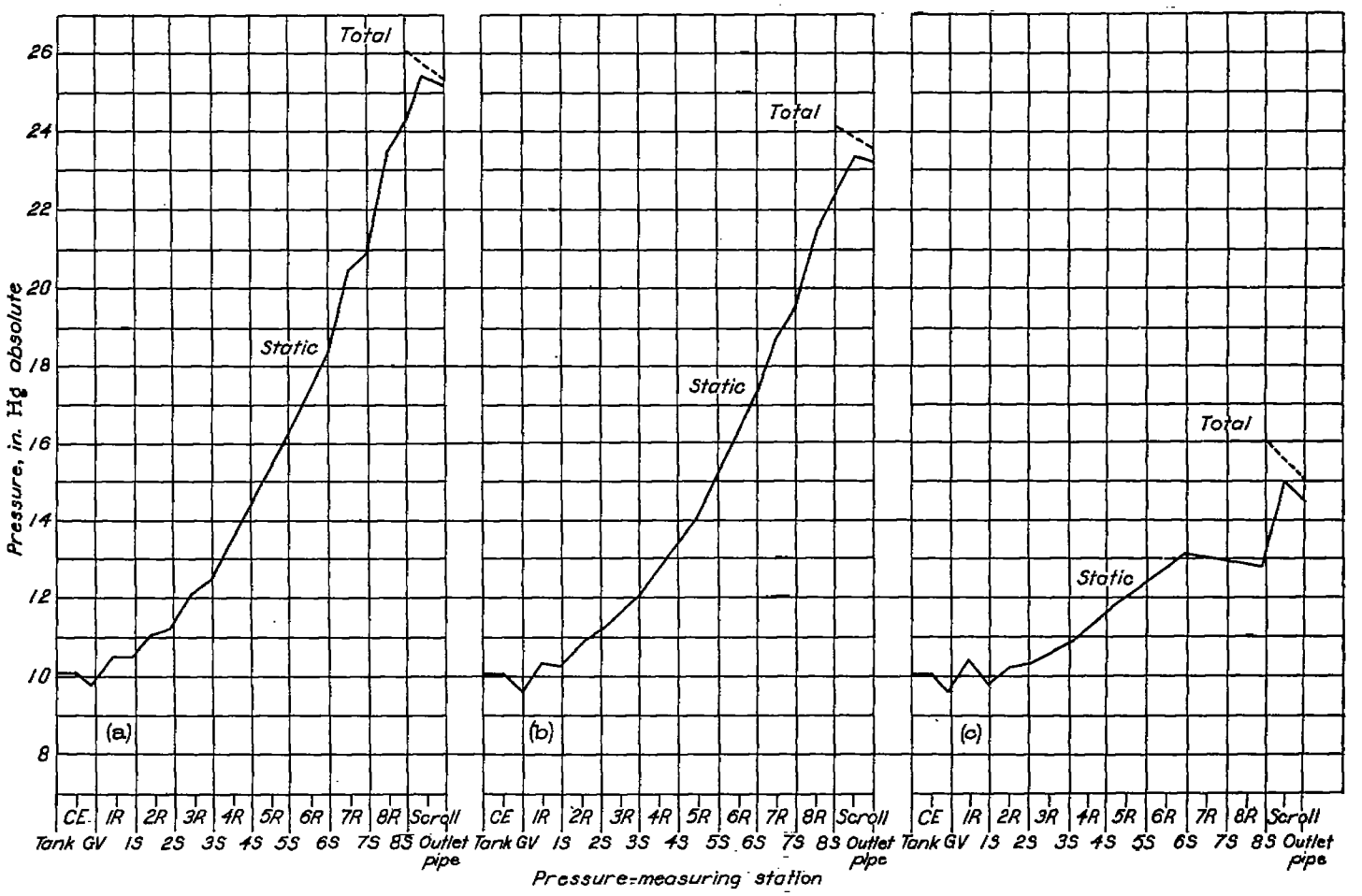

(a) Q_1/n, 0.334; η_T, 0.740. (b) Q_1/n, 0.434; η_T, 0.782. (c) Q_1/n, 0.462; η_T, 0.567.

FIGURE 19.—Pressure distribution from inlet tank to outlet pipe with stator blades reset for 75 percent of design speed at load coefficient of 0.48. Compressor Mach number, 0.7; inlet-air temperature, 0° F; inlet-air pressure, 10.16 inches mercury absolute. Pressure measurements made after each blade row. CE, at compressor entrance; GV, after guide vanes; R, after rotor blades; S, after stator blades.

low velocities at the casing wall behind the guide vanes and possibly backflow at the tips of the rotor blades.

At the low flow of $Q_1/n=0.105$ (fig. 20 (a)), an appreciable over-all pressure ratio was obtained although the pressure distribution indicated unsatisfactory flow conditions. Almost all the pressure rise was obtained in the stator rows, indicating excessive stalling of the rotor blades. A peculiar condition observed for the entrance guide vanes was that the pressure behind the guide vanes was substantially higher than in the tank ahead of the vanes. This result cannot be attributed to experimental error inasmuch as it was consistently observed in all the tests in which the compressor Mach number and the air flow were both low. The fact that the static pressures behind the guide vanes were greater than the total pressure ahead of the guide vanes might seem to violate Bernoulli's equation. This apparent paradox may be accounted for by flow separation along the casing inasmuch as Bernoulli's equation applies only to flow along a single streamline. At the outer part of the rotor blades, the air would be merely carried around with the blades, which would produce an appreciable pressure gradient from hub to tip. The large pressure difference across the entrance guide vanes at the casing is possible because of the excessively high losses that would accompany any upstream flow through the guide vanes at the tip as the angle of attack for such flow would be extremely high.

Performance based on total-pressure surveys after last stator row.—At each Mach number for both stator-blade resettings, total-pressure surveys were made directly behind the last row of stator blades. In figure 21, the performance characteristics of the compressor with reset stator blades are shown based on total-pressure surveys at the compressor

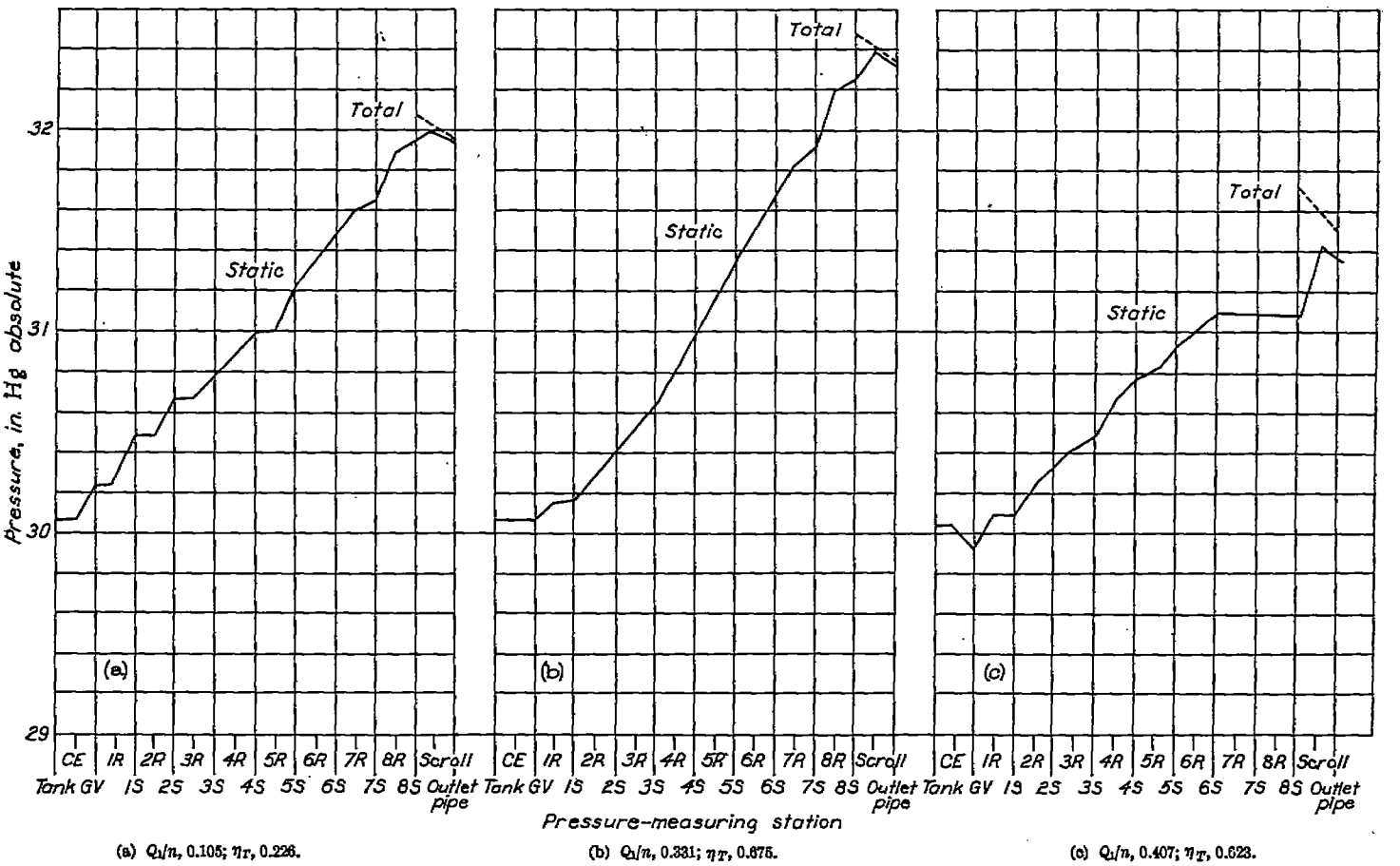

(a) Q_1/n, 0.105; η_T, 0.226. (b) Q_1/n, 0.331; η_T, 0.675. (c) Q_1/n, 0.407; η_T, 0.623.

FIGURE 20.—Pressure distribution from inlet tank to outlet pipe with stator blades reset for 75 percent of design speed at load coefficient of 0.48. Compressor Mach number, 0.2; approximately standard sea-level inlet-air conditions. Pressure measurements made after each blade row. CE, at compressor entrance; GV, after guide vanes; R, after rotor blades; S, after stator blades.

outlet and on total-pressure readings in the outlet pipe. This figure shows that considerably higher efficiencies and pressure ratios are attained over the compressor proper than over the compressor and the scroll collector. The maximum efficiencies based on the total-pressure surveys obtained in these tests were 80.5 percent for the first resetting and 87 percent for the second resetting at a compressor Mach number of 0.8. At the Mach number for which the blades were reset (0.726), peak efficiencies of approximately 80.5 and 85 percent were attained for the first and second resettings, respectively.

At each Mach number the spread between the over-all efficiency of the compressor-scroll combination and the efficiency of the compressor proper increases as the flow increases. This result may be attributed to the large increase in the velocity of the air entering the scroll with a corresponding increase in scroll losses.

SUMMARY OF EXPERIMENTAL RESULTS

From an investigation of the effect of stator-blade resetting on the performance of the NACA eight-stage axial-flow compressor, the following results were obtained:

1. When the stator blades were reset for 75 percent of design speed at two different load coefficients, considerable improvement in the peak efficiencies was obtained for both stator-blade resettings at compressor speeds appreciably below the design speed.

2. A difference of 20 to 30 percent in the peak-efficiency flows for the two stator-blade resettings was obtained.

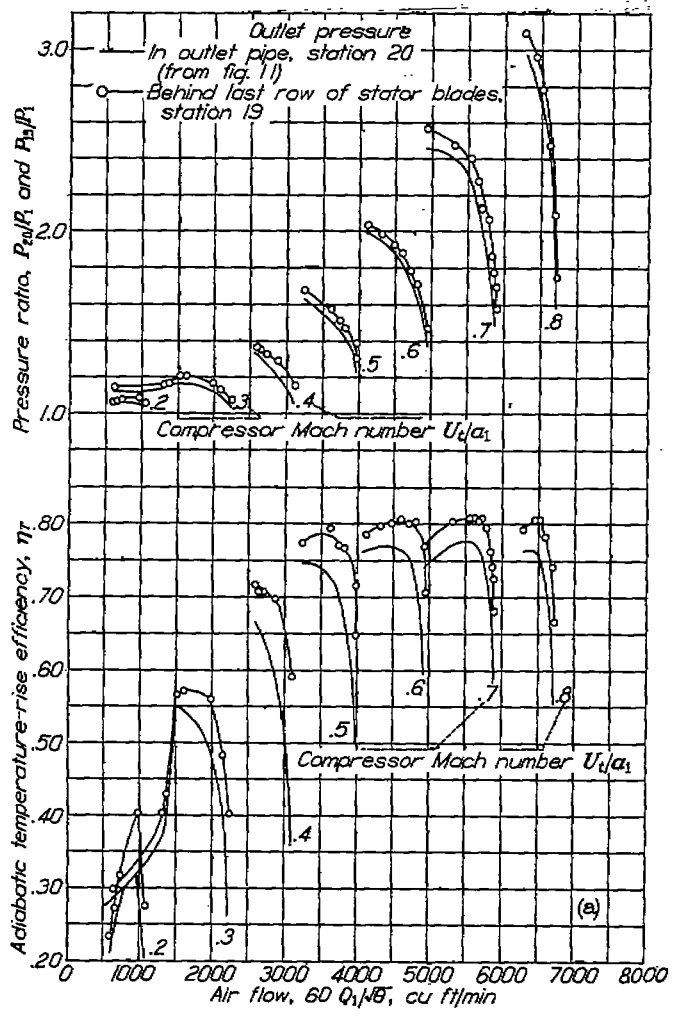

(a) Load coefficient, 0.48.

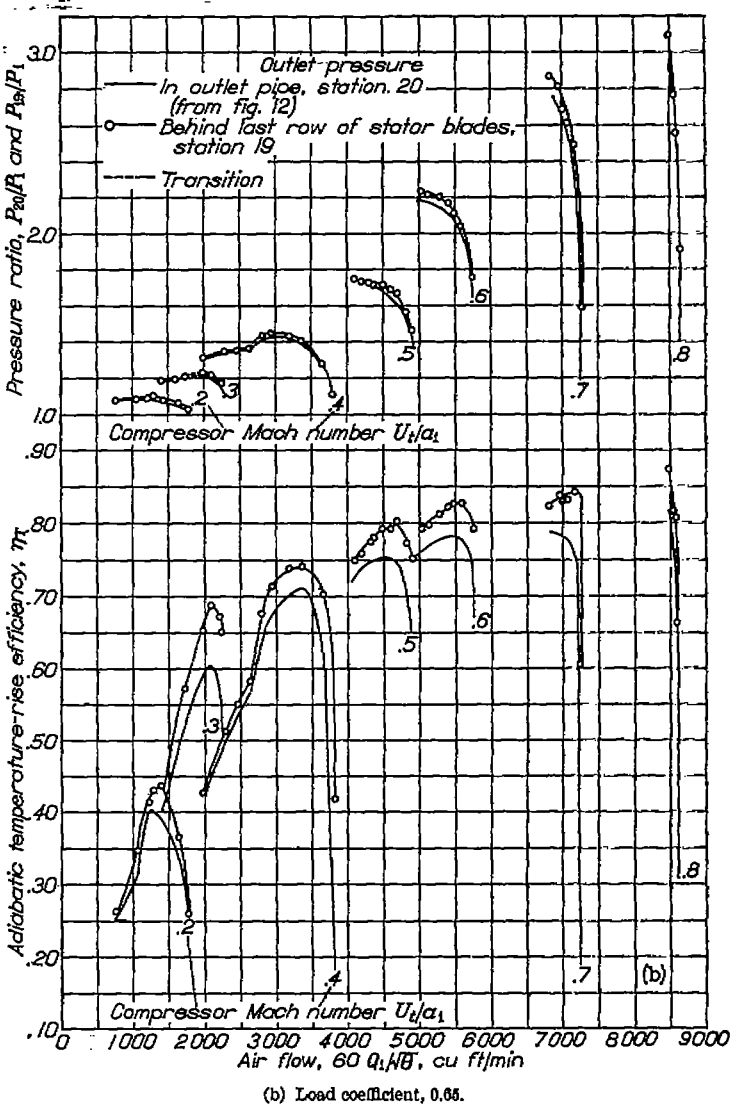

(b) Load coefficient, 0.65.

FIGURE 21.—Comparison of performance characteristics of axial-flow compressor based on total-pressure measurements in outlet pipe and behind last row of stator blades. Stator blades reset for 75 percent of design speed.

3. Peak pressure ratios were increased with the stator blades reset for a load coefficient of 0.65 and were substantially the same as for the design blade setting with the stator blades reset for a load coefficient of 0.48.

4. Inlet-air conditions were found to have a very large effect on the adiabatic temperature-rise efficiency at low compressor Mach numbers, which is believed to be caused by heat-transfer and Reynolds number effects.

5. No definite surging of the compressor was observed below a compressor Mach number of 0.4; instead, a sudden transition to a lower pressure ratio occurred when the flow was decreased appreciably below the peak-efficiency point.

CONCLUSIONS

By the adjustment of only the stator-blade angles, substantial improvement of the peak efficiencies can be obtained at speeds below the design speed; and, by the use of different blade settings, the flows for peak efficiency can be varied so as to extend greatly the useful flow range of the compressor.

AIRCRAFT ENGINE RESEARCH LABORATORY,
NATIONAL ADVISORY COMMITTEE FOR AERONAUTICS,
CLEVELAND, OHIO, *December 29, 1944.*

APPENDIX A

ENTRANCE-GUIDE-VANE CALCULATIONS

An exact calculation of the flow at all radii throughout a multistage compressor, which involves problems of considerable difficulty, has not been attempted in the calculation procedure. For the entrance guide vanes, however, more detailed calculations of the flow conditions at different radii have been made because the small value of the hub-tip diameter ratio at the compressor inlet makes the radial distribution especially important.

Velocity distribution behind entrance guide vanes.—An approximation of the radial distribution of air velocity and velocity components behind the guide vanes can be obtained if it is assumed that radial equilibrium has been established at this point (station 3, fig. 1). Although this assumption is not strictly true because, in general, some radial flow will exist at this station, the assumption should give a much better approximation than the assumption of constant axial velocity at all radii. The condition for radial equilibrium is

$$\frac{\partial p}{\partial r}=\frac{\rho V_w^2}{r} \tag{25}$$

For the present calculation, losses through the entrance guide vanes will be neglected in order that Bernoulli's equation

$$\frac{1}{2}V^2+\int\frac{dp}{\rho}=C \tag{26}$$

with the same constant C at all radii can be used. This equation can then be differentiated with respect to r, which gives

$$V\frac{\partial V}{\partial r}+\frac{1}{\rho}\frac{\partial p}{\partial r}=0 \tag{27}$$

The whirl-velocity component in equation (25) can be eliminated by the relation

$$V_w=V\sin\beta \tag{28}$$

and the pressure can be eliminated by use of equation (27) to obtain

$$-\frac{1}{V}\frac{\partial V}{\partial r}=\frac{\sin^2\beta}{r} \tag{29}$$

which, when integrated with respect to the radius, gives

$$\log\left(\frac{V_t}{V}\right)=-\int_r^{r_t}\frac{\sin^2\beta}{r}\,dr \tag{30}$$

The indicated integration can be carried out if β is known as a function of r. For compressors in which β is constant with respect to the radius, as is approximately the case with the NACA eight-stage axial-flow compressor, equation (30) can be directly integrated to obtain

$$\frac{V}{V_t}=\left(\frac{r}{r_t}\right)^{-\sin^2\beta} \tag{31}$$

Equation (30) gives the distribution of the resultant velocity as a function of the radius. The distribution of the whirl component and the axial component of velocity can also be readily obtained when β is known as a function of the radius.

Mean velocity behind guide vanes.—The continuity equation applied to the flow between stations 1 and 3 (fig. 1) can be written

$$\int\rho_1 v_1\,2\pi r dr=\int\rho_3 v_3\,2\pi r dr \tag{32}$$

where the integrations are made over the flow passages at these two stations. Because station 1 is chosen where the cross-sectional area is large and the velocity negligible and the fluid is assumed to be homogeneous, the density at station 1 is constant and the first integral can be replaced by $\rho_1 Q_1$. The right side of equation (32) can be expressed

$$\int\rho_3 v_3\,2\pi r dr=\rho_{3,f}\int v_3\,2\pi r dr=\rho_{3,f}Q_3 \tag{33}$$

where $\rho_{3,f}$ is the flow-average density. Equation (32) then becomes

$$Q_3=Q_1\frac{\rho_1}{\rho_{3,f}} \tag{34}$$

The condition for constant total enthalpy between stations 1 and 3 can be written as (assuming V_1 to be negligible)

$$1-\frac{t_3}{t_1}=\frac{V_3^2}{2gJc_p t_1} \tag{35}$$

By use of the polytropic relation between temperature and density, the perfect-gas laws, and the relation for the velocity of sound, the following density ratio is obtained:

$$\frac{\rho_3}{\rho_1}=\left[1-\frac{\gamma-1}{2}\left(\frac{V_3}{a_1}\right)^2\right]^{\frac{1}{m'-1}} \tag{36}$$

If this equation is applied at the mean radius and if the density at the mean radius is assumed to be equal to flow-average density, equation (36) can be substituted in equation (34) to give

$$Q_1=Q_3\left[1-\left(\frac{\gamma-1}{2}\right)\left(\frac{V_3}{a_1}\right)_{mr}^2\right]^{\frac{1}{m'-1}} \tag{37}$$

Throughout the rest of appendix A, the mean-radius subscript mr will be omitted and all quantities will refer to the mean radius unless otherwise indicated.

If the axial velocity at the mean radius $V_3\cos\beta_3$ is assumed to be equal to the average axial velocity Q_3/A_3, then V_3/a_1 may be replaced by $Q_3/(a_1A_3\cos\beta_3)$. If this substitution is made and equation (37) is divided by $a_1A_3\cos\beta_3$, the following relation is obtained:

$$\frac{Q_1}{a_1A_3\cos\beta_3}=\frac{Q_3}{a_1A_3\cos\beta_3}\left[1-\left(\frac{\gamma-1}{2}\right)\left(\frac{Q_3}{a_1A_3\cos\beta_3}\right)^2\right]^{\frac{1}{m'-1}} \tag{38}$$

which is the same as equation (7). The value of V_3/a_1 at the mean radius is given by equation (9) and can be obtained at other radii by use of equation (30).

Angles of attack and lift coefficients on first row of rotor blades.—The angle of attack and the lift coefficient on the first row of rotor blades can now be calculated as follows: The relative whirl component of velocity at any radius is obtained from the absolute whirl component by the relation

$$\frac{W_{w,3}}{a_1}=\frac{U_3}{a_1}-\frac{V_{w,3}}{a_1} \qquad (39)$$

and the relative air angle ϕ_3 is obtained from the relation

$$\tan \phi_3=\frac{W_{w,3}/a_1}{v_3/a_1} \qquad (40)$$

The angle of attack α_3 (relative to the entrance velocity W_3) is given by

$$\alpha_3=\phi_3-\psi_R \qquad (41)$$

The angle of the air leaving the first row of rotor blades ϕ_4 is obtained from the relation

$$\phi_4=(1-K)\phi_3+K\psi_R+K\alpha_0 \qquad (42)$$

and the lift coefficient is obtained from equations (22) and (23).

APPENDIX B

DERIVATION OF EQUATIONS FOR POLYTROPIC FLOW THROUGH TYPICAL STAGE

For the row of stator blades the energy equation is

$$\frac{V_i^2}{2}-\frac{V_{i+1}^2}{2}=gJc_p t_i\left(\frac{t_{i+1}}{t_i}-1\right) \tag{43}$$

For compression with a polytropic exponent m, this relation can be written

$$\frac{V_i^2}{2}-\frac{V_{i+1}^2}{2}=\frac{\gamma}{\gamma-1}\frac{p_i}{\rho_i}\left[\left(\frac{\rho_{i+1}}{\rho_i}\right)^{m-1}-1\right]$$
$$=\frac{a_i^2}{\gamma-1}\left[\left(\frac{\rho_{i+1}}{\rho_i}\right)^{m-1}-1\right] \tag{44}$$

which, when solved for ρ_{i+1}/ρ_i, gives

$$\frac{\rho_{i+1}}{\rho_i}=\left\{1+\frac{\gamma-1}{2}\left(\frac{a_1}{a_i}\right)^2\left[\left(\frac{V_i}{a_1}\right)^2-\left(\frac{V_{i+1}}{a_1}\right)^2\right]\right\}^{\frac{1}{m-1}} \tag{45}$$

For the following row of rotor blades the energy equation is

$$\frac{W_{i+1}^2}{2}-\frac{W_{i+2}^2}{2}+\frac{U_{i+2}^2}{2}-\frac{U_{i+1}^2}{2}=gJc_p t_{i+1}\left(\frac{t_{i+2}}{t_{i+1}}-1\right) \tag{46}$$

where U is the rotor velocity at the radius midway between the hub and the casing at the station indicated by the subscript. The terms containing U are required because of the centrifugal-force field existing in the rotating frame of reference; the effect of these terms is generally quite small in axial-flow compressors where the change in radius from station to station is small. The density ratio for the row of rotor blades may be obtained in a manner similar to that for the stator blades, the result being

$$\frac{\rho_{i+2}}{\rho_{i+1}}=\left\{1+\frac{\gamma-1}{2}\left(\frac{a_1}{a_{i+1}}\right)^2\left[\left(\frac{W_{i+1}}{a_1}\right)^2-\left(\frac{W_{i+2}}{a_1}\right)^2+\left(\frac{U_{i+2}}{a_1}\right)^2-\left(\frac{U_{i+1}}{a_1}\right)^2\right]\right\}^{\frac{1}{m-1}} \tag{47}$$

In order to use equations (45) and (47) together with the relations for turning angle (equations (17) and (18)) and the continuity relation, it is convenient to express the air velocities in terms of the axial components and the relative air angles. Equation (45) for the stator blades becomes

$$\frac{\rho_{i+1}}{\rho_i}=\left\{1+\frac{\gamma-1}{2}\left(\frac{a_1}{a_i}\right)^2\left[\frac{(v_i/a_1)^2}{\cos^2\beta_i}-\frac{(v_{i+1}/a_1)^2}{\cos^2\beta_{i+1}}\right]\right\}^{\frac{1}{m-1}} \tag{48}$$

and equation (47) for the rotor blades becomes

$$\frac{\rho_{i+2}}{\rho_{i+1}}=\left\{1+\frac{\gamma-1}{2}\left(\frac{a_1}{a_{i+1}}\right)^2\left[\frac{(v_{i+1}/a_1)^2}{\cos^2\phi_{i+1}}-\frac{(v_{i+2}/a_1)^2}{\cos^2\phi_{i+2}}+\left(\frac{U_{i+2}}{a_1}\right)^2-\left(\frac{U_{i+1}}{a_1}\right)^2\right]\right\}^{\frac{1}{m-1}} \tag{49}$$

The density ratio can be eliminated from these equations by use of the continuity equation, which for the stator blades is

$$\frac{\rho_{i+1}}{\rho_i}=\frac{v_i}{v_{i+1}}\frac{A_i}{A_{i+1}}$$

to obtain

$$\frac{v_i}{a_1}=\frac{v_{i+1}}{a_1}\frac{A_{i+1}}{A_i}\left\{1+\frac{\gamma-1}{2}\left(\frac{a_1}{a_i}\right)^2\left[\frac{(v_i/a_1)^2}{\cos^2\beta_i}-\frac{(v_{i+1}/a_1)^2}{\cos^2\beta_{i+1}}\right]\right\}^{\frac{1}{m-1}} \tag{50}$$

and

$$\frac{v_{i+1}}{a_1}=\frac{v_{i+2}}{a_1}\frac{A_{i+2}}{A_{i+1}}\left\{1+\frac{\gamma-1}{2}\left(\frac{a_1}{a_{i+1}}\right)^2\left[\frac{(v_{i+1}/a_1)^2}{\cos^2\phi_{i+1}}-\frac{(v_{i+2}/a_1)^2}{\cos^2\phi_{i+2}}+X\right]\right\}^{\frac{1}{m-1}} \tag{51}$$

where

$$X=\left(\frac{U_{i+2}}{a_1}\right)^2-\left(\frac{U_{i+1}}{a_1}\right)^2$$

which are equations (19) and (24), respectively.

REFERENCES

1. Sinnette, John T., Jr., Schey, Oscar W., and King, J. Austin: Performance of NACA Eight-Stage Axial-Flow Compressor Designed on the Basis of Airfoil Theory. NACA Rep. No. 758, 1944.
2. Betz, A.: Axial Superchargers. NACA TM No. 1073, 1944.
3. Seippel, C.: The Development of the Brown-Boveri Axial Compressor. Brown Boveri Rev., Brown, Boveri & Co., Ltd. (Switzerland), vol. XXVII, no. 5, May 1940, pp. 108–113.
4. White, William Monroe: American Hydraulic Turbines. Mech. Eng., vol. 52, no. 4, April 1930, pp. 390–395.
5. Daugherty, R. L.: Hydraulics. McGraw-Hill Book Co., Inc., 1937, p. 407.
6. Keller, Curt: The Theory and Performance of Axial-Flow Fans. (Adapted for the use of fan designers by Lionel S. Marks and John R. Weske.) McGraw-Hill Book Co., Inc., 1937.
7. Keller, C.: Multi-Stage Axial Flow Fans of Today and Yesterday Design. Escher Wyss News, vol. XI, no. 2, April–June 1938, pp. 39–44.
8. Bell, E. Barton: Test of a Single-Stage Axial-Flow Fan. NACA Rep. No. 729, 1942.
9. Meldahl, A.: End Losses of Turbine Blades. Jour. Am. Soc. Naval Eng., vol. 54, no. 3, Aug. 1942, pp. 454–466. (Reprinted from Brown Boveri Rev., Brown, Boveri & Co., Ltd. (Switzerland), vol. XXVIII, no. 11, Nov. 1941, pp. 356–361.)
10. Harris, R. G., and Fairthorne, R. A.: Wind Tunnel Experiments with Infinite Cascades of Aerofoils. R. & M. No. 1206, British A. R. C., 1928.
11. Shimoyama, Yoshinori: Experiments of Rows of Aerofoils for Retarded Flow. Trans. Soc. Mech. Eng. (Japan), vol. 3, no. 13, Nov. 1937, pp. 334–344. (Japanese text with English summary, pp. S–83—S–84.)
12. Kantrowitz, Arthur, and Daum, Fred L.: Preliminary Experimental Investigation of Airfoils in Cascade. NACA CB, July 1942.
13. Bogdonoff, Seymour M., and Bogdonoff, Harriet E.: Blade Design Data for Axial-Flow Fans and Compressors. NACA ACR No. L5F07a, 1945.
14. Weske, John R., and Marble, Frank E.: Characteristics of Airfoils in a Cylindric Axial-Flow Grid. Jour. Aero. Sci., vol. 10, no. 8, Oct. 1943, pp. 289–294.
15. Zimney, Charles M., and Lappi, Viola M.: Data for Design of Entrance Vanes from Two-Dimensional Tests of Airfoils in Cascade. NACA ACR No. L5G18, 1945.
16. King, J. Austin, and Regan, Owen W.: Performance of NACA Eight-Stage Axial-Flow Compressor at Simulated Altitudes. NACA ACR No. E4L21, 1944.
17. Ruden, P.: Investigation of Single-Stage Axial Fans. NACA TM No. 1062, 1944.

TABLE I—EFFECT OF ENTRANCE-GUIDE-VANE SETTINGS ON ANGLES OF ATTACK AND THEORETICAL LIFT COEFFICIENTS ON FIRST ROW OF ROTOR BLADES AT DIFFERENT LOAD COEFFICIENTS AND RADII FOR NACA AXIAL-FLOW COMPRESSOR

Load coefficient	Guide-vane setting [1] (deg)	Air angle at exit of guide vanes [2] (deg)	Angle of attack on first row of rotor blades, α_3 (deg)			Theoretical lift coefficient on first row of rotor blades [3]		
			Hub	Mean radius	Tip	Hub	Mean radius	Tip
0.28	27	43	35.1	25.6	13.0	2.15	3.02	3.45
	37	53	32.1	25.0	13.0	1.91	2.91	3.44
	47	63	25.8	23.7	12.8	1.46	2.72	3.87
0.38	27	43	28.1	21.7	10.4	1.62	2.43	2.72
	37	53	22.3	20.4	10.3	1.25	2.25	2.67
	47	63	7.1	17.4	9.6	.48	1.88	2.49
0.48	37	53	10.3	15.0	7.2	0.62	1.61	1.94
	47	63	−18.6	8.7	5.5	−.42	1.01	1.62
	57	73	−90.5	−34.6	−8.5	−2.89	−1.33	.24
0.65	27	43	5.5	9.0	2.3	0.41	1.03	1.05
	37	53	−14.0	3.2	.7	−.28	.57	.80
0.70	17	33	11.7	9.9	1.6	0.68	1.11	0.93
	27	43	.9	6.3	.6	.23	.80	.78
	37	53	−21.2	−1.1	−1.6	−.50	.28	.48

[1] The guide-vane setting is the angle between the tangent to the concave surface of the vane and the axis of the compressor. Because there is no twist in these vanes, this angle is the same at all radii. The design setting was 27°.

[2] The air angle behind the guide vanes was experimentally determined for the design setting and was found to be approximately 43° at all radii. Because of the high solidity of the entrance guide vanes, it was assumed that for other settings the change of the air angle from the design value was the same as the change of the guide-vane setting; that is, K in equation (6) was assumed equal to 1.0.

[3] The lift coefficients (based on assumption that blades do not stall) are used to indicate the favorable or adverse conditions existing at the entrance to the rotor blades rather than actual lift coefficients that would be expected.

TABLE II—SUMMARY OF CALCULATIONS ON RESETTING OF STATOR BLADES OF NACA EIGHT-STAGE AXIAL-FLOW COMPRESSOR FOR 75 PERCENT OF DESIGN SPEED (COMPRESSOR MACH NUMBER, 0.726)

Blade row	Blade angle at mid-span (deg)	Increase of blade angle over design angle (deg)	Lift coefficient at mid-span	Static-pressure ratio at mid-span	Diffusion-velocity ratio [1] at mean radius	Relative Mach number ahead of blade row at mean radius	Ratio of rotor velocity to axial component of air velocity at mean radius
Load coefficient, 0.28							
Entrance guide vanes	37.0	10.0	1.08	0.985	1.88	0.07	-----
First rotor [2]	55.4	0	2.91	1.143	.28	.48	7.3
First stator	84.9	35.9	.28	1.013	.95	.49	7.2
Second rotor	47.9	0	.80	1.014	.81	.16	6.7
Second stator	88.1	35.6	.38	1.028	.91	.52	6.3
Third rotor	45.3	0	.80	1.014	.82	.18	5.8
Third stator	80.6	35.3	.42	1.035	.89	.53	5.4
Fourth rotor	43.1	0	.77	1.014	.84	.21	5.0
Fourth stator	77.3	35.0	.42	1.044	.86	.54	5.0
Fifth rotor	42.3	0	.72	1.015	.83	.24	4.3
Fifth stator	73.3	30.7	.48	1.051	.84	.53	4.0
Sixth rotor	41.6	0	.71	1.018	.83	.28	3.7
Sixth stator	68.2	28.1	.55	1.054	.83	.53	3.4
Seventh rotor	40.1	0	.71	1.020	.84	.32	3.1
Seventh stator	63.2	25.5	.53	1.057	.81	.53	2.9
Eighth rotor	37.7	0	.71	1.029	.78	.35	2.8
Eighth stator	56.9	19.4	.70	1.091	.69	.53	2.8
Load coefficient, 0.38							
Entrance guide vanes	37.0	10.0	1.08	0.975	1.89	0.10	-----
First rotor [2]	55.4	0	2.25	1.114	.41	.45	5.3
First stator	79.2	30.2	.32	1.015	.94	.46	5.2
Second rotor	47.9	0	.83	1.019	.80	.22	4.9
Second stator	46.7	29.2	.47	1.035	.87	.50	4.6
Third rotor	45.3	0	.79	1.019	.82	.24	4.3
Third stator	78.1	27.9	.51	1.041	.86	.51	4.0
Fourth rotor	43.1	0	.74	1.019	.85	.27	3.7
Fourth stator	67.9	25.6	.55	1.055	.82	.52	3.4
Fifth rotor	42.3	0	.73	1.025	.82	.32	3.2
Fifth stator	62.0	19.4	.62	1.059	.79	.51	3.0
Sixth rotor	41.6	0	.71	1.029	.82	.36	2.8
Sixth stator	55.1	15.0	.69	1.058	.79	.51	2.6
Seventh rotor	40.1	0	.71	1.034	.83	.41	2.4
Seventh stator	48.4	10.7	.68	1.061	.79	.51	2.3
Eighth rotor	37.7	0	.72	1.051	.77	.45	2.2
Eighth stator	45.2	7.7	.70	1.078	.72	.52	2.2

TABLE II—SUMMARY OF CALCULATIONS ON RESETTING OF STATOR BLADES OF NACA EIGHT-STAGE AXIAL-FLOW COMPRESSOR FOR 75 PERCENT OF DESIGN SPEED (COMPRESSOR MACH NUMBER, 0.726)—Concluded

Blade row	Blade angle at mid-span (deg)	Increase of blade angle over design angle (deg)	Lift coefficient at mid-span	Static-pressure ratio at mid-span	Diffusion-velocity ratio [1] at mean radius	Relative Mach number ahead of blade row at mean radius	Ratio of rotor velocity to axial component of air velocity at mean radius
Load coefficient, 0.48							
Entrance guide vanes	47.0	20.0	1.37	0.926	2.00	0.12	-----
First rotor [2]	55.4	0	1.00	1.041	.74	.33	3.0
First stator	69.5	20.5	.46	1.024	.88	.43	3.3
Second rotor	47.9	0	.80	1.029	.80	.31	3.5
Second stator	65.7	18.2	.62	1.014	.82	.48	3.4
Third rotor	45.3	0	.80	1.031	.81	.34	3.2
Third stator	60.0	14.7	.70	1.054	.80	.49	3.0
Fourth rotor	43.1	0	.79	1.036	.82	.38	2.8
Fourth stator	52.1	9.8	.77	1.065	.76	.50	2.6
Fifth rotor	42.3	0	.78	1.048	.79	.44	2.5
Fifth stator	46.9	4.3	.75	1.060	.78	.50	2.3
Sixth rotor	41.6	0	.68	1.045	.83	.47	2.2
Sixth stator	41.1	.9	.73	1.049	.82	.50	2.0
Seventh rotor	40.1	0	.61	1.042	.86	.51	1.9
Seventh stator	38.3	−4.4	.71	1.050	.83	.52	1.8
Eighth rotor	37.7	0	.62	1.071	.80	.56	1.7
Eighth stator	31.4	−6.1	.70	1.008	.77	.53	1.7
Load coefficient, 0.65							
Entrance guide vanes	27.0	0	0.82	0.918	1.57	0.17	-----
First rotor [2]	55.4	0	1.04	1.069	.72	.45	3.0
First stator	55.6	6.7	.60	1.025	.86	.40	2.9
Second rotor	47.9	0	.84	1.047	.78	.40	2.8
Second stator	53.7	6.2	.70	1.041	.82	.45	2.6
Third rotor	45.3	0	.72	1.039	.84	.42	2.5
Third stator	48.5	3.2	.70	1.042	.83	.48	2.3
Fourth rotor	43.1	0	.63	1.036	.87	.45	2.2
Fourth stator	40.4	−1.9	.70	1.047	.83	.49	2.0
Fifth rotor	42.3	0	.57	1.043	.87	.51	1.9
Fifth stator	33.1	−9.6	.70	1.041	.86	.50	1.8
Sixth rotor	41.6	0	.51	1.043	.89	.57	1.7
Sixth stator	24.9	−15.2	.70	1.028	.91	.52	1.5
Seventh rotor	40.1	0	.47	1.045	.91	.64	1.4
Seventh stator	15.5	−22.2	.70	1.025	.93	.56	1.3
Eighth rotor	37.7	0	.52	1.115	.81	.73	1.3
Eighth stator	14.5	−23.1	.70	1.053	.86	.57	1.3
Load coefficient, 0.70							
Entrance guide vanes	27.0	0	0.82	0.939	1.58	0.18	-----
First rotor [2]	55.4	0	.81	1.055	.79	.44	2.8
First stator	52.7	3.7	.50	1.017	.90	.39	2.7
Second rotor	47.9	0	.70	1.042	.83	.42	2.5
Second stator	48.5	1.0	.70	1.037	.83	.45	2.4
Third rotor	45.3	0	.65	1.040	.86	.45	2.3
Third stator	42.8	−2.5	.70	1.038	.85	.48	2.1
Fourth rotor	43.1	0	.58	1.037	.89	.50	2.0
Fourth stator	34.2	−8.2	.70	1.041	.85	.50	1.8
Fifth rotor	42.3	0	.52	1.016	.88	.56	1.7
Fifth stator	26.4	−16.3	.70	1.034	.89	.52	1.6
Sixth rotor	41.6	0	.47	1.046	.91	.63	1.5
Sixth stator	18.0	−23.1	.70	1.017	.95	.54	1.4
Seventh rotor	40.1	0	.45	1.052	.82	.72	1.3
Seventh stator	8.6	−29.1	.70	1.009	.98	.59	1.2
Eighth rotor	37.7	0	.50	1.115	.80	.83	1.2
Eighth stator	8.6	−28.9	.70	1.045	.89	.60	1.2

[1] The diffusion velocity ratio is the ratio of the relative velocity leaving to the relative velocity entering the row of blades.

[2] The calculations are based on the assumption that the blades do not stall. For the first row of rotor blades, where a high lift coefficient is sometimes obtained by the calculation method presented herein, the blades would probably stall, making the actual lift coefficient and pressure ratio considerably less than the values indicated for this row of blades.